

OBTAINING UNIFORM SINGULAR VALUES OF
AUGMENTED SYSTEMS USING LQG/LTR

By

BRIAN DWAYNE O'DELL

Bachelor of Science

Oklahoma State University

Stillwater, Oklahoma

1993

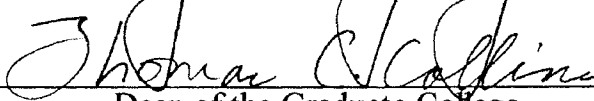
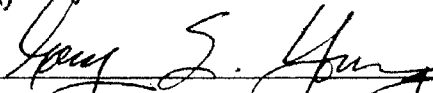
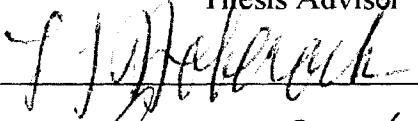
Submitted to the Faculty of the
Graduate College of the
Oklahoma State University
in partial fulfillment of
the requirements for
the Degree of
MASTER OF SCIENCE
December, 1994

OBTAINING UNIFORM SINGULAR VALUES OF
AUGMENTED SYSTEMS USING LQG/LTR

Thesis Approved:



Thesis Adviser



Dean of the Graduate College

PREFACE

There are well-developed methods for attaining either low or high frequency singular value agreement for general systems using LQG/LTR design techniques. For systems that have been augmented with additional dynamics, it has been previously shown that simultaneous low and high frequency agreement, or balancing, is possible, although singular values at mid-range frequencies were not directly adjusted. This paper presents two methods for obtaining simultaneous singular value agreement over all frequencies for the target loop. The procedure requires that the augmented systems have free integrators acting on each of the inputs. Two examples are included which illustrate the techniques and demonstrate how to utilize preexisting free integrators within the system.

I sincerely thank my major advisor, Dr. Eduardo Misawa, for his supervision of this project. Through his encouragement, I was able to develop a simple idea I had during class into the thesis presented here.

This material is based upon work supported under a National Science Foundation Graduate Research Fellowship and a Du Pont Company Graduate Fellowship in Mechanical Engineering.

TABLE OF CONTENTS

Chapter	Page
I. INTRODUCTION	1
Background of Multivariable Control.....	2
The Problem.....	2
Objective of the Research	3
Significance and Contribution of the Research	3
Scope and Limitations	4
II. REVIEW OF THE LITERATURE	5
Balancing Singular Values of Nominal Plants.....	7
Low and High Frequency Ranges.....	7
Arbitrary Frequency Location	7
Balancing Singular Values of Augmented Plants	8
Previous Work.....	8
Present Study	8
III. LQG/LTR DESIGN FOR AUGMENTED SYSTEMS	10
Augmented System Dynamics.....	10
Filter Loop Transfer Function.....	12
Standard Solution Method.....	14
Improved Method 1: Null Vectors and Mapping Matrices.....	15
Improved Method 2: Exact Solution.....	18
Summary of Design Procedure	18
IV. EXAMPLES	21
Example 1: Translational Mass-Spring System.....	21
Example 2: Lightly-Damped Rotating Arm.....	41
V. CONCLUSIONS.....	51
BIBLIOGRAPHY	52

Chapter	Page
APPENDIX.....	54
Derivation of Formula	54
Proof of Exact Solution	55

LIST OF FIGURES

Figure	Page
1. Diagram of Mass-Spring System.....	22
2. Singular Values of Original System.....	25
3. Block Diagram of Un-Augmented System.....	29
4. Block Diagram of Free Integrators.....	29
5. Singular Values of Filter Loop using Nominal H	32
6. Singular Values of Filter Loop using Improved H	33
7. Transient Response of System using Improved H.....	34
8. Transient Response of System using Nominal H.....	35
9. Transient Behavior of Control Forces using Improved H.....	36
10. Transient Behavior of Control Forces using Nominal H.....	36
11. Transient Response using Nominal H with Accurate Model.....	38
12. Transient Response using Nominal H with Faulty Model.....	39
13. Transient Response using Improved H with Accurate Model.....	40
14. Transient Response using Improved H with Faulty Model	40
15. Singular Values of Nominal Plant.....	43
16. Singular Values of Target Loop Transfer Function.....	47
17. Singular Values of Target Loop Using Approximate H	48

Figure	Page
18. Transient Response of System Using Exact Filter Matrix.....	49
19. Transient Response of System Using Approximate H.....	50

CHAPTER I

INTRODUCTION

One of the primary functions of the engineer is to use the basic principles of science and mathematics to develop solutions to problems. The effectiveness of a solution is often defined in terms of its shortcomings, such as excessive cost or low reliability. These limitations identify new problems to solve, perhaps by using less expensive materials or more rugged components. With each improvement in one area, however, there may be trade-offs in another. For instance, more resilient materials might improve the reliability of mechanical parts, but might also increase the overall cost.

The same can be said of control schemes: those processes which cause a system to operate in a desired manner. For single-input/single-output (SISO) systems, a number of control methods have been developed, including lead/lag compensators, feedback pole placement, and optimal control. The first of these is a dynamic process, which is more complicated than the constant gain feedback control of the latter two. The second method allows the user to select a gain which will provide the desired rise time, overshoot, and other time response properties. But while the behavior of the system after pole placement may be ideal, the amount of control effort used to effect this performance may be excessive. In this case, the final method might be the best option, as it attempts to balance the performance of the system with the required control effort.

Background of Multivariable Control

There are similar options to consider when designing control schemes for multi-input/multi-output (MIMO) systems. However, while techniques such as pole placement are still available, they are considerably more difficult. This complexity is a result of the fact that, since these systems have more than one input and more than one output, the input to output transfer functions are matrix quantities. For each element in the matrix, there is likely to be a different set of poles and zeros. Additionally, the traditional concept of zeros no longer applies, since the zeros of the scalar matrix elements have no apparent relevance to the zeros of the complete system.

The importance of the order of the matrices in the transfer function representation also creates difficulty, since the mathematical components of a MIMO transfer function cannot simply be rearranged as with a scalar SISO system. Finally, and perhaps most importantly, MIMO systems have multiple input to output amplitude ratios. Therefore, while the Bode magnitude plot of an SISO transfer function consists of a single trace indicating amplitude ratio as a function of frequency, MIMO systems have multiple traces, showing at the very least the maximum and minimum amplitude ratios that could be expected for a given input signal frequency.

The Problem

The ability to manipulate these minimum and maximum ratios, or singular values (since they come from the singular values of the system transfer function), leads to a popular method for designing linear multivariable controllers: the traditional linear-

quadratic Gaussian/loop transfer recovery (LQG/LTR) technique. This topic will be discussed in greater detail shortly, but suffice it to say that the method reduces a complicated sequence of matrices and loops to a simpler, single-loop equation.

Previous work in the field of LQG/LTR has shown that it is possible to obtain nearly identical singular values over limited frequency ranges. As opposed to singular values which are significantly different at a given frequency, identical singular values improve system performance by ensuring that the system outputs will behave similarly for that frequency. It would therefore be desirable to obtain identical singular values over as great a frequency range as possible.

Objective of the Research

This research was designed to identify means of obtaining balanced singular values over a greater frequency range than had previously been shown to be possible. Initially, improvement was sought at those frequency locations where the difference in maximum and minimum singular values was the greatest. It was thought that by decreasing this maximum spread the agreement over all frequencies would generally improve. Further investigation showed that it was possible to obtain singular value agreement over all frequencies for certain systems.

Significance and Contribution of the Research

As a potential refinement of the existing design procedures, this paper introduces two new ideas to the field of LQG/LTR. The first concept is that singular values of transfer

function matrices can not only be made identical (as has been previously shown) but can be made to equal those of a desirable first-order transfer function shape. The second concept is that, in forcing the singular value traces to a single, first-order form, the singular values can be made identical not just for limited frequency ranges (the focus of previous work) but for all frequencies.

Scope and Limitations

This research was based on systems which have either preexisting and/or augmented free integrators acting on each of the inputs. It is a common specification in control system design to have zero steady-state error, which requires the addition of free integrators to obtain at least a type 1 system. Free integrators which are a physical component of the system can cause problems, as the addition of too many of these elements will cause as many problems as having too few. Therefore, the examples included show how to isolate these preexisting poles at the origin and use them advantageously.

This paper does not, however, directly discuss how to match singular values to anything other than the Bode form of a free integrator, as it is unlikely that a non-zero augmented pole location should be specified. If the need should arise however, it is possible to adapt the equations derived in the Appendix to suit such a need. Furthermore, the methods presented here cannot, in general, be used with non-augmented systems, unless there are already the same number of free integrators in the system as there are inputs.

CHAPTER II

REVIEW OF THE LITERATURE

The loop transfer recovery (LTR) theory for multivariable system control evolved from the search for a dynamic compensator which would provide good command following and stability robustness properties. Its development can be traced to one of the most basic MIMO control techniques (also used frequently with SISO systems), the linear quadratic regulator (LQR), which involves the selection of an "optimal" control gain matrix, K . This control method provides certain inherent benefits, including nominal stability and stability robustness. However, while LQR ensures a stable system, it is not designed for command following roles. Even when modified to the form of the LQ-Servo (which permits output feedback, but requires that the gain matrix be broken into two parts), the performance of a MIMO system to a reference input was poor.

When state estimation was added to a system, the combined dynamics of this filter loop and the control loop were found to have an interesting structure, called the model based compensator (MBC). This control structure was promising because it allowed for non-zero reference inputs to the system. Furthermore, the Separation Theorem permitted the gain matrices to be developed independently in fictitious control and filter loops. The gain matrices could be selected using pole placement (which, if the poles had negative real components, ensures nominal stability), linear quadratic Gaussian (LQG) techniques (ensuring both nominal stability and stability robustness), or any other method.

One drawback to the MBC is that, even if stability robustness is guaranteed for the separate controller and filter loops, the same may not be true for the combined MBC/plant structure. However, it was found that if LQG techniques were used to select both the gain matrices, the singular values of the overall transfer function would approach those of a simpler target loop (Doyle and Stein 1981). As discussed by Stein and Athans (1987), the objective of LTR is to shape a target loop (either the filter loop, $C(sI-A)^{-1}H$, or the control loop, $K(sI-A)^{-1}B$, where A , B , and C are from the standard state-space form, (1)),

$$\begin{aligned}\dot{x}(t) &= Ax(t) + Bu(t) \\ y(t) &= Cx(t)\end{aligned}\tag{1}$$

and then attempt to recover its singular value loop shapes by properly selecting the remaining gain matrix (K or H , respectively). Therefore, if the “targeted” filter loop is designed as a linear Luenberger state estimator and the control gain matrix chosen so as to recover this loop, then the complete control system will exhibit the estimator’s stability robustness properties.

A limitation with this and any other MIMO control technique is that the singular values of the nominal system are generally spread apart over the entire frequency range. With SISO systems, the response of the system to inputs of different frequencies is represented using the Bode diagram. For such systems, the Bode magnitude plot consists of a single line representing the amplitude ratio of system output to system input as a function of frequency.

With multi-input/multi-output systems, multiple output to input amplitude ratios occur. Furthermore, the values of these ratios will vary for a given frequency if the direction of the input vector changes (i.e., making only one of the inputs non-zero, making

all inputs the same magnitude, etc.). For this reason, the singular value plot is used to describe the input/output amplitude ratio for MIMO systems. These diagrams show how the singular values of the transfer function matrix vary with frequency and indicate (at minimum) the upper and lower bounds of these quantities.

Balancing Singular Values of Nominal Plants

Low and High Frequency Ranges

The difference between the maximum and minimum singular values of a system can be large near points of resonance and nearly zero at other locations. A wide spread between upper and lower bounds can degrade system performance and limit the designer's ability to specify crossover frequency or other desired characteristics. However, it is possible to obtain agreement of singular values for some frequencies when LQG/LTR is used. For nominal (un-augmented) system plants, methods have been presented for 'balancing' singular values either at low or high frequencies (Birdwell et al. 1984). With these cases, the procedure is to select the gain matrix such that the target loop transfer function approaches the identity matrix as frequency tends to zero or infinity, respectively.

Arbitrary Frequency Location

Birdwell and Laub (1987) presented a third alternative in which singular values are balanced at an arbitrary frequency location. This technique is similar to the low and high frequency balancing methods except that the transfer function matrix is evaluated at a fixed frequency location. The authors noted that being able to balance singular values at

an arbitrary frequency location provided additional design flexibility, but did not suggest an algorithm for selecting the frequency where matching would provide the best results.

Balancing Singular Values of Augmented Plants

Previous Work

Greater flexibility in manipulating the singular values occurs when additional dynamics are augmented to the nominal plant. A typical example is when free integrators are added to each of the inputs such that the closed-loop system has zero steady-state error. For such a system, it has been shown that the linear-quadratic Gaussian (LQG) target loop can be made to exhibit balanced singular values at both low and high frequencies, simultaneously (Martin et al. 1986). This was achieved by partitioning the gain matrix into two components: one which was identified as dominating singular value behavior at low frequencies, and another which dominated at high frequencies. These submatrices were then optimized to provide balanced singular values in their frequency range. However, while results at low and high frequencies are generally good, singular values at mid-range frequencies (often of greater interest to the control system designer) often show little improvement.

Present Study

This paper shows that it is possible to obtain balanced singular values over all frequencies at the same time. The next chapter presents two methods for obtaining this, both of which utilize the partitioning of the gain matrix suggested by Martin et al (1986).

The first method applies the suggestion by Birdwell and Laub (1987) of evaluating the transfer function at an arbitrary frequency location, but, by introducing the concepts of null vectors and mapping matrices, shows that matching can be performed at several frequency locations. If enough matches are performed, it has been determined that the singular values will be identical for all frequencies. The second method presents an exact solution to the matching problem in a single equation, eliminating the need for null vectors and mapping matrices.

CHAPTER III

LQG/LTR DESIGN FOR AUGMENTED SYSTEMS

Before introducing the methods for selection of the gain matrices, the state-space representation of augmented systems is first developed, following the procedure by Martin et al. (1986). The equations have been modified to initially include cases where stable poles are augmented to the systems dynamics.

Augmented System Dynamics

Begin with the nominal plant model, which is of the standard state-space form shown below, where A_p is of dimension $(n \times n)$, B_p is $(n \times m)$, C_p is $(m \times n)$, and $m < n$.

$$\begin{aligned}\dot{x}_p(t) &= A_p x_p(t) + B_p u_p(t) \\ y(t) &= C_p x_p(t)\end{aligned}\tag{2}$$

Also, let $G_p(s)$ represent the transfer function matrix of the nominal system, given by equation (3). In (3) and subsequent equations, note that $s = j\omega$, and that 'I' refers to the identity matrix.

$$G_p(s) = C_p (sI - A_p)^{-1} B_p\tag{3}$$

Now suppose that each the inputs to the nominal plant is augmented with an additional, stable pole, resulting in (4).

$$\dot{u}_p = (-pI)u_p + u_a\tag{4}$$

The transfer matrix representing these augmented dynamics is given by (5).

$$G_a(s) = I / (s + p)\tag{5}$$

The combined transfer matrix for the nominal and augmented plant dynamics is given by $G(s) = G_p(s)G_a(s)$. This transfer function can be represented in the standard state-space form $C(sI-A)^{-1}B$, where these matrices are defined as follows:

$$\begin{aligned} C &= [\emptyset \quad C_p], \\ A &= \begin{bmatrix} -pI & \emptyset \\ B_p & A_p \end{bmatrix}, \\ B &= \begin{bmatrix} I \\ \emptyset \end{bmatrix} \end{aligned} \quad (6)$$

Also, it can be shown (Brogan 1991) that the inverse of $(sI-A)$ is given by

$$(sI - A)^{-1} = \begin{bmatrix} I/(s+p) & \emptyset \\ (sI - A_p)^{-1}B_p/(s+p) & (sI - A_p)^{-1} \end{bmatrix} \quad (7)$$

In this new system, (6), C is of dimension $[m \times (n + m)]$, A is $[(n + m) \times (n + m)]$, and B is $[(n + m) \times m]$.

With the state-space representation thus defined, the method for selecting the gain matrix of the target loop can now be described. This paper uses the filter loop as the target loop of the system, as opposed to the method where the compensator loop is the target. However, since the two methods are duals, the process should be adaptable to the latter case. Once the filter loop is determined, the control gain matrix must be computed using the following form of the Control Analytical Ricatti Equation (CARE) (9), a requirement for loop transfer recovery

$$K = (1/\rho)B'S \quad (8)$$

$$\emptyset = A'S + SA + C'C - (1/\rho)SBB'S \quad (9)$$

where ρ is a free parameter. Note that the filter matrix, H , does not influence the value of the controller gain matrix, K .

Filter Loop Transfer Function

At this point, the scope has been limited to the case where free integrators are added to the system, and the equations that follow are derived for that specific case. As indicated earlier, this common problem results from the specification of zero steady-state error. The equations that follow could likely be adapted to fit a more general pole location, $-p$. However, the formula would be considerably more involved than that presented here and would not be as useful, since it is uncommon to specify a non-zero augmented pole location. It is therefore left to the reader to adapt the equations included in the Appendix to a more general pole location should the need arise.

With the filter loop chosen as the target loop for the system, the gain matrix, H , is selected using the Kalman Filter method. The procedure first requires the introduction of fictitious white noise terms into system (6),

$$\begin{aligned}\dot{x}(t) &= Ax(t) + L\zeta(t) \\ y(t) &= Cx(t) + \theta(t)\end{aligned}\tag{10}$$

where $\zeta(t)$ has covariance I , and $\theta(t)$ has covariance μI . Since the noise terms do not represent real disturbances, the matrix L and the constant μ are not fixed but act as free parameters that may be selected to meet design criteria.

The actual values of L and μ are therefore not as important as the effect they have on H , the filter gain matrix. With the constant gain Kalman Filter method, the relationship between the filter gain and the free parameters is given by the solution to the Filter Algebraic Ricatti Equation (FARE) (12).

$$H = (1/\mu)\Sigma C'\tag{11}$$

$$\dot{\theta} = A\Sigma + \Sigma A' + LL' - (1/\mu)\Sigma C' C\Sigma \quad (12)$$

Beginning with equation (12), it has been shown (Kwakernaak and Sivan 1972) that the singular values of the Kalman Filter loop, $C(sI-A)^{-1}H$, are given by

$$\sigma_i[I + G_{KF}(j\omega)] = \sqrt{1 + (1/\mu)\sigma_i^2[C(j\omega I - A)^{-1}L]} \quad (13)$$

which, for $\mu \ll 1$, reduces to

$$\sigma_i[G_{KF}(j\omega)] \approx (1/\sqrt{\mu})\sigma_i[C(j\omega I - A)^{-1}L] \quad (14)$$

If the filter open loop transfer function matrix, $C(sI-A)^{-1}L$ (henceforth referred to as $G_{FOL}(s)$), approaches some multiple of the identity matrix for a given frequency, then its singular values will become equal for that frequency.

From (14), it can be seen that identical singular values of $G_{FOL}(s)$ imply identical singular values of $G_{KF}(s)$, as well. The problem, then, lies in finding the gain matrix, L , which will result in identical singular values for the filter open loop transfer matrix, shown in (15).

$$G_{FOL}(s) = [\emptyset \quad C_p] \begin{bmatrix} I/s & \emptyset \\ (sI - A_p)^{-1}B_p/s & (sI - A_p)^{-1} \end{bmatrix} L \quad (15)$$

Applying the suggestion by Martin et al (1986) to partition L into low and high frequency submatrices results in (16), where L_L is $(m \times m)$ and L_H is $(n \times m)$.

$$G_{FOL}(s) = C_p(sI - A_p)^{-1}B_p L_L / s + C_p(sI - A_p)^{-1}L_H \quad (16)$$

As frequency tends to zero, the extra free integrator in the first, or 'low frequency,' term of (16) means that this part of the equation will dominate. As frequency tends to infinity, this same free integrator causes the first term to die out faster than the second, allowing the 'high frequency' term to dominate.

Standard Solution Method

Since free integrators were augmented to the system inputs, singular values will be balanced if the matrix L is selected so that $G_{FOL}(s)$ approaches I_m/s , where the subscript “m” denotes the dimension of the identity matrix as $(m \times m)$. (If poles at $-p$ were added, then $I_m/(s+p)$ would be used, although L_L would not dominate at low frequencies, and the equations would need to be adjusted accordingly.) Assuming that A_p contains no free integrators (or they have somehow been moved out, as in the example which follows), then for low frequencies, (16) becomes

$$I_m / s = -C_p A_p^{-1} B_p L_L / s - C_p A_p^{-1} L_H \quad (17)$$

Since, as stated earlier, the low frequency term will dominate as s approaches $j0$, then (17) reduces to

$$I_m / s = -C_p A_p^{-1} B_p L_L / s \quad (18)$$

The solution for L_L is a unique, $(m \times m)$ matrix and is given by

$$L_L = -[C_p A_p^{-1} B_p]^{-1} \quad (19)$$

For high frequencies, (16) becomes

$$I_m / s = C_p B_p L_L / s^2 + C_p L_H / s \quad (20)$$

Since, as s approaches $j\infty$, $1/s \gg 1/s^2$, (20) reduces to

$$I_m / s = C_p L_H / s \quad (21)$$

Because C_p is not square, a unique solution does not exist for L_H . In fact, since C_p is $(m \times n)$, and $m < n$, then an infinite number of solutions exist. The typical method for finding L_H has been to compute the minimum norm solution of (21), as shown in (22).

$$L_H = C_p^{-1} (C_p C_p^T)^{-1} \quad (22)$$

Improved Method 1: Null Vectors and Mapping Matrices

From linear algebra, it is known that null vectors will accompany any minimum norm solution. Letting the columns of a matrix N_1 represent the null vectors of C_p , then by definition

$$C_p N_1 = \emptyset \quad (23)$$

This, in turn, implies that

$$C_p (L_H + N_1 M) = C_p L_H \quad (24)$$

where M is an arbitrary mapping matrix representing any linear combination of the columns of N_1 . Also, recall that N_1 will not affect L_L due to the partitioning of the L matrix. The point of this is that adding null vectors of C_p to the high frequency component of L will not degrade singular value agreement at either low or high frequencies. They may therefore be used to augment the high frequency component of L to obtain more balanced singular values at mid-range frequencies.

The first step in the process of improving agreement is to select a frequency at which the singular values are to be balanced. Typically, the best way to do this is to first compute H from (11) and (12) using L_L and L_H as the L matrix. Then, plot the singular values of $G_{KF}(s)$ and locate the frequency of maximum spread, ω_1 , which is generally near a resonant frequency ($j\omega_1$ may not, however, be one of the poles of A_p , since $(sI - A_p)$ must remain invertible.) The next step is to determine which linear combination of the null

vectors, represented by a mapping matrix, M_1 , results in the best match. This is given by the solution of M_1 in the following equation

$$I / j\omega_1 = C_p (j\omega_1 I - A_p)^{-1} B_p L_L / j\omega_1 + C_p (j\omega_1 I - A_p)^{-1} (L_H + N_1 M_1) \quad (25)$$

which may be rewritten as

$$C_p (j\omega_1 I - A_p)^{-1} N_1 M_1 = I / j\omega_1 - C_p (j\omega_1 I - A_p)^{-1} B_p L_L / j\omega_1 - C_p (j\omega_1 I - A_p)^{-1} L_H \quad (26)$$

(In practice, this generally yields a complex L matrix. However, the LQG process will return a real H matrix.)

The method for finding M_1 will vary depending on the number of rows and columns of the matrix coefficient of M_1 , and whether or not they are linearly independent. To account for all the possibilities that might occur, it is recommended that the Moore-Penrose generalized inverse be used for computing all mapping matrices. This pseudoinverse effectively computes the unique inverse of a matrix if it is square and nonsingular, the minimum norm solution if its rows are linearly independent, or the least squares solution if its columns are linearly independent. The method also accommodates cases where the matrix may not be full rank (neither the set of columns nor the set of rows are linearly independent). A number of numerical procedures exist for computing this pseudoinverse, including singular value decomposition (SVD), Gram-Schmidt orthogonalization, and Gauss-Jordan elimination. The reader is referred to Arthur (1972) for a more detailed discussion of the pseudoinverse and the methods available for computing it.

Referring again to (26), it can be seen that a new, more limited set of null vectors exists, and is given by

$$N_2 = \text{null} \left\{ C_p (j\omega_1 I - A_p)^{-1} N_1 \right\} \quad (27)$$

The matrix N_2 represents the linear combination of the columns of N_1 which was not used to improve singular value agreement at ω_1 . The set of vectors given by the columns of $N_1 N_2$ can therefore be used to balance singular values at another frequency without degrading agreement at low frequencies, high frequencies, or near ω_1 . The procedure for selecting the new frequency, ω_2 , is the same as before, except that a new L matrix, given by the submatrices L_L and $(L_H + N_1 M_1)$, is used to compute the new H. The mapping, M_2 , which gives the best singular value agreement at the new frequency location is given by the solution to the following equation.

$$I_m / j\omega_2 = C_p (j\omega_2 I - A_p)^{-1} B_p L_L / j\omega_2 + C_p (j\omega_2 I - A_p)^{-1} (L_H + N_1 (M_1 + N_2 M_2)) \quad (28)$$

This process of finding mapping matrices and remaining null vectors continues until all null vectors are used. At this point, it is necessary to include a word of caution regarding the calculation of the null vectors. The matrix coefficient of M_i is often poorly conditioned. However, it may not be so bad that a computer program will recognize all the null vectors. It is therefore up to the user to recognize these additional null vectors, in many cases made easier by rounding the matrix's elements off to, say, the fourth or fifth decimal place, and include them in the calculation of the next mapping matrix.

The final result of this sequential process is an L matrix of the form shown in equation (29).

$$L = \begin{bmatrix} L_L \\ L_H + N_1 (M_1 + N_2 (M_2 + N_3 (M_3 + \dots + N_{k-1} (M_{k-1} + N_k M_k) \dots))) \end{bmatrix} \quad (29)$$

Improved Method 2: Exact Solution

Initially, Method 1 was used to improve singular value agreement at specific frequencies. It was later determined that if enough steps were performed such that all null vectors were used, identical singular values occurred at all frequencies. In fact, this result is readily obtained by selecting the L_H submatrix using (30).

$$L_H = A_p^{-1} B_p (C_p A_p^{-1} B_p)^{-1} \quad (30)$$

The derivation of (30) and proof that $G_{FOL}(s)$ will equal $1/s$ for all frequencies is included in the Appendix.

With either method, the resulting L matrix provides the basic form of the loop shape. The other free parameter, the scalar μ , can now be selected to provide the desired crossover frequency of $G_{KI}(s)$, as with standard LQG/LTR design methodology.

Summary of Design Procedure

The design procedure for an LQG/LTR controller can be summarized in the following steps:

1. Develop a linearized state-space representation of the system (the A , B , C , and D matrices).
2. If necessary, augment the system with additional dynamics such that only one free integrator is acting on each of the inputs.
3. Choose L (using either Method 1 or Method 2) to give the desirable loop shape (i.e., obtain singular value matching).

4. Choose μ to give the proper crossover frequency and to ensure good agreement between the real $C(sI-A)^{-1}H$ and fictional $C(sI-A)^{-1}L$ loops.
5. Choose ρ small enough so that the combined controller/plant transfer function approaches that of the target filter loop, $C(sI-A)^{-1}H$ (i.e., obtain loop transfer recovery.)

There are no real guidelines for selecting the free parameters in steps 4 and 5.

However, it should be noted from (13) that, so long as the singular values of $G_{FOL}(s)$ are identical, the singular values of $G_{KF}(s)$ will be as well, regardless of the choice of μ . So, the only real issue is the desired crossover point of the transfer function, which effectively specifies the system's speed of response.

As for the selection of ρ , a smaller value will increase the upper limit of the frequency range where loop transfer recovery occurs, but will also create large elements in the K matrix, resulting in greater control effort. As noted previously, the crossover frequency of the open loop transfer function affects many of the closed-loop time response characteristics, so it is important that singular value agreement be maintained to this point. However, it is unlikely that one would design a control system with a crossover point lower than the frequency of any expected reference signals (trying to force a system to respond faster than it is designed for would create inherent steady-state error), so it might not be necessary to try to maintain match in this high-frequency region. A good rule-of-thumb, therefore, might be to select ρ small enough to obtain a good match just beyond the crossover frequency, but no further. In other words, choosing ρ as large as possible while still maintaining match at crossover should provide good transient response while

minimizing the control effort. The following section contains two examples that demonstrate this procedure and the two techniques presented for obtaining uniform singular values.

CHAPTER IV

EXAMPLES

Example 1: Translational Mass-Spring System

Consider a system consisting of three masses and two springs, with force inputs F_1 acting on mass 1 and F_3 acting on mass 3, as shown in Figure 1, which might be a lumped parameter model of a more complicated physical system. An LQG/LTR servo is to be designed for this system which will meet the following specifications:

- Zero steady-state error for arbitrary constant command (reference) inputs and disturbances,
- Target loop singular values should be identical,
- Cross-over frequency should be about 10 rad/sec.

The first specification can be met by applying a free integrator to each of the control inputs, the second by applying the technique for selecting the filter gain matrix as described earlier, and the third by manipulating the free parameter, μ , from (12).

Before proceeding with the design, the system shown in Figure 1 must be described mathematically. Assuming that the damping is proportional to velocity, then a linear differential equation may be written for each mass, using Newton's second law of motion.

$$\begin{aligned} F_1 - b_1 \dot{x}_1 - k_{12}(x_1 - x_2) &= m_1 \ddot{x}_1 \\ -b_2 \dot{x}_2 + k_{12}(x_1 - x_2) - k_{23}(x_2 - x_3) &= m_2 \ddot{x}_2 \\ F_3 - b_3 \dot{x}_3 + k_{23}(x_2 - x_3) &= m_3 \ddot{x}_3 \end{aligned} \quad (31)$$

Suppose that the physical constants have the following numerical values:

$$\begin{aligned}
m_i &= 1 \text{ kg} \\
k_{ij} &= 1 \text{ N/m} \\
b_i &= 0.1 \text{ N}\cdot\text{s/m}
\end{aligned}
\tag{32}$$

The set of equations, (31), may be rewritten as:

$$\begin{aligned}
F_1 - 0.1\dot{x}_1 - x_1 + x_2 &= \ddot{x}_1 \\
-0.1\dot{x}_2 - 2x_2 + x_1 + x_3 &= \ddot{x}_2 \\
F_3 - 0.1\dot{x}_3 - x_3 + x_2 &= \ddot{x}_3
\end{aligned}
\tag{33}$$

At this point, it might be necessary to normalize the equations as with standard LQG/LTR procedure, although the system used here does not necessitate this.

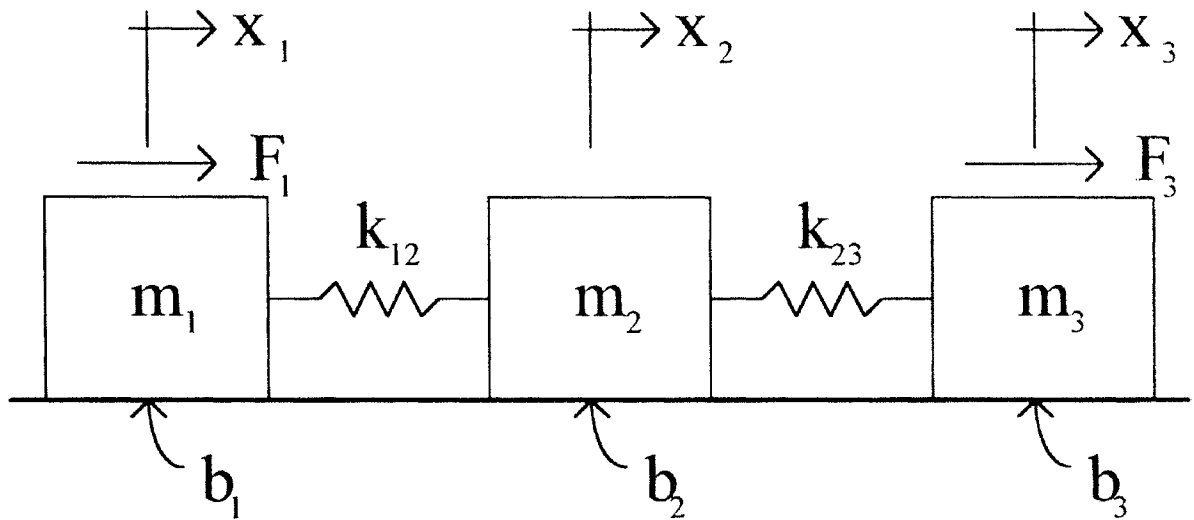


Figure 1. Diagram of Mass-Spring System

Let the variables z_1 through z_6 represent the state variables of the system according to (34), where v_i is the velocity of mass i .

$$\begin{aligned}
z_1 &= x_1 \\
z_2 &= \dot{x}_1 = v_1 \\
z_3 &= x_2 \\
z_4 &= \dot{x}_2 = v_2 \\
z_5 &= x_3 \\
z_6 &= \dot{x}_3 = v_3
\end{aligned} \tag{34}$$

Also, let y_1 and y_2 represent the system outputs, defined by (35).

$$\begin{aligned}
y_1 &= x_1 = z_1 \\
y_2 &= x_3 - x_1 = z_5 - z_1
\end{aligned} \tag{35}$$

The state equations may now be written in matrix form, given by (36).

$$\begin{aligned}
\begin{bmatrix} \dot{z}_1 \\ \dot{z}_2 \\ \dot{z}_3 \\ \dot{z}_4 \\ \dot{z}_5 \\ \dot{z}_6 \end{bmatrix} &= \begin{bmatrix} 0 & 1 & 0 & 0 & 0 & 0 \\ -1 & -0.1 & 1 & 0 & 0 & 0 \\ 0 & 0 & 0 & 1 & 0 & 0 \\ 1 & 0 & -2 & -0.1 & 1 & 0 \\ 0 & 0 & 0 & 0 & 0 & 1 \\ 0 & 0 & 1 & 0 & -1 & -0.1 \end{bmatrix} \begin{bmatrix} z_1 \\ z_2 \\ z_3 \\ z_4 \\ z_5 \\ z_6 \end{bmatrix} + \begin{bmatrix} 0 & 0 \\ 1 & 0 \\ 0 & 0 \\ 0 & 0 \\ 0 & 0 \\ 0 & 1 \end{bmatrix} \begin{bmatrix} F_1 \\ F_3 \end{bmatrix} \\
\begin{bmatrix} y_1 \\ y_2 \end{bmatrix} &= \begin{bmatrix} 1 & 0 & 0 & 0 & 0 & 0 \\ -1 & 0 & 0 & 0 & 1 & 0 \end{bmatrix} \begin{bmatrix} z_1 \\ z_2 \\ z_3 \\ z_4 \\ z_5 \\ z_6 \end{bmatrix}
\end{aligned} \tag{36}$$

As will be seen in a moment, these equations are not yet in a usable form. Therefore, the A, B, and C matrices will be designated with the subscript, “n”, for nominal plant, to distinguish them from the plant matrices (subscript “p”) which will actually be used in the design.

The poles of (36), given by the eigenvalues of A_n , are

$$\begin{aligned}
& -0.05 \pm j1.7313 \\
& -0.05 \pm j0.9987 \\
& -0.1 \\
& 0.0
\end{aligned}
\tag{37}$$

Transmission zeros of the system were computed to be

$$-0.05 \pm j1.4133 \tag{38}$$

and correspond to the case where mass 2 (the position of which is not measured) acts as a vibrational damper for the rest of the system. The effects of these poles and transmission zeros on the behavior of the system are shown in Figure 2, the singular value plot of (36).

The two complex pole pairs create resonant peaks near 1.0 and 1.7 rad/sec. The complex transmission zero pair causes a trough in the lower singular value plot at 1.4 rad/sec.

These distortions increase the spread between upper and lower singular values. Additional disparity is created by the presence of the pole at the origin, which is seen as the -20db/dec slope of the upper bound at low frequencies.

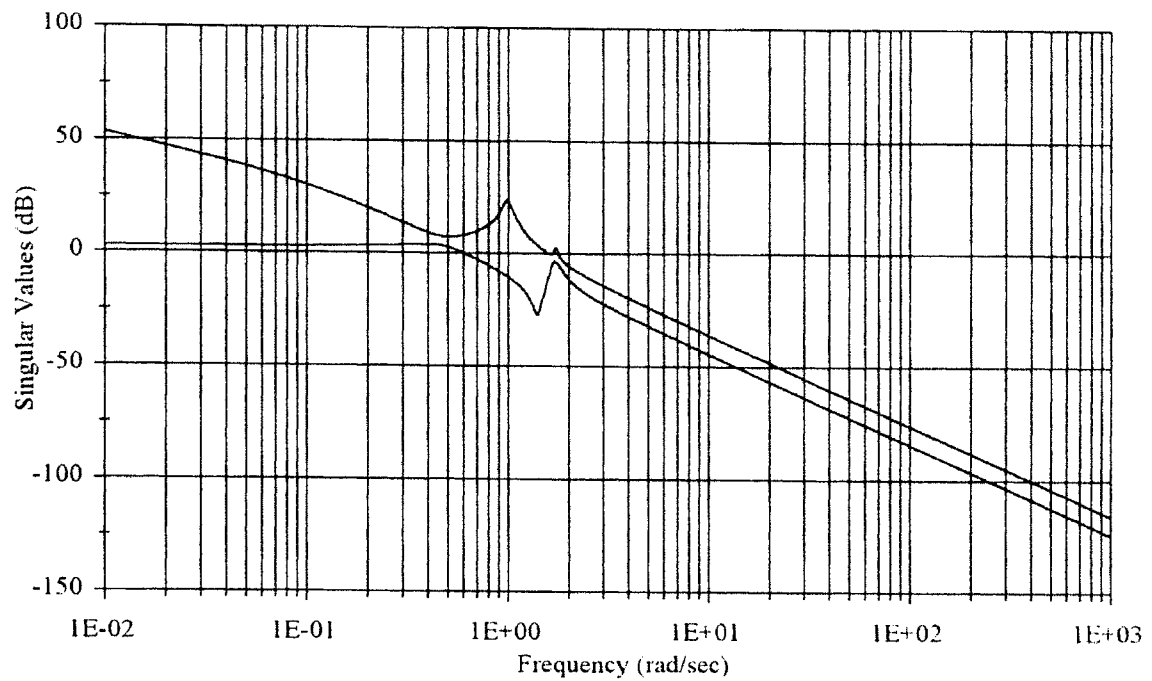


Figure 2. Singular Values of Original System

With most systems, the state-space representation of the augmented system could now be written using (5), with $p = 0$. However, the existence of the pole at the origin in this system means that some matrix manipulation must first be performed. Due to this free integrator, the present A_n matrix is not invertible, such that low frequency singular value matching cannot be performed via (19), nor could high frequency matching using (30). In terms of Figure 2, the upper bound tends to infinity as frequency tends to zero, while the lower bound tends to a finite quantity, meaning that a gain of infinity on the lower would be necessary to match singular values. This effect relates to the suggestion that identical, first order poles must be acting on each of the inputs to obtain identical singular values over all frequencies.

Since the upper bound already has a pole at zero, it is reasonable to attempt to add just one more free integrator which will operate on the lower bound, providing zero steady-state error. To do this, the existing free integrator must be isolated from the original system to determine which of the inputs (or linear combination thereof) it operates on. The new free integrator could then be applied to the remaining input (or linearly independent combination of inputs) to obtain the desired result.

By the definition of a free integrator, one of the states (or, again, a linear combination of them) is simply the integral of a combination of the inputs. Therefore, there should be some combination of z_i 's that will result in a zero row in the A_n matrix. This is guaranteed by the fact that a zero eigenvalue implies that the rows of A_n are not linearly independent. It can be shown that the temporary state variables given by (39) isolate the free integrator in this manner.

$$\begin{bmatrix} z'_1 \\ z'_2 \\ z'_3 \\ z'_4 \\ z'_5 \\ z'_6 \end{bmatrix} = \begin{bmatrix} 0.1 & 1 & 0.1 & 1 & 0.1 & 1 \\ 1 & 0 & 0 & 0 & 0 & 0 \\ 0 & 1 & 0 & 0 & 0 & 0 \\ 0 & 0 & 0 & 1 & 0 & 0 \\ 0 & 0 & 0 & 0 & 1 & 0 \\ 0 & 0 & 0 & 0 & 0 & 1 \end{bmatrix} \begin{bmatrix} z_1 \\ z_2 \\ z_3 \\ z_4 \\ z_5 \\ z_6 \end{bmatrix} \quad (39)$$

Notice that z_2 is not a unique element in the z' coordinates. The selection of which state variable to eliminate was somewhat arbitrary, although an attempt was made to maintain z_1 and z_5 in their original form, since these are measured outputs.

Designating the above mapping matrix from z to z' as G_1 , system (36) in the new coordinates is given by

$$\begin{aligned}\dot{z}' &= G_1 A_n G_1^{-1} z' + G_1 B_n u \\ y &= C_n G_1^{-1} z'\end{aligned}\quad (40)$$

which results in the state-space representation

$$\begin{aligned}\dot{z}' &= \begin{bmatrix} 0 & 0 & 0 & 0 & 0 & 0 \\ 0 & 0 & 1 & 0 & 0 & 0 \\ 10 & -20 & -10.1 & -10 & -1 & -10 \\ -20 & 3 & 20 & 19.9 & 3 & 20 \\ 0 & 0 & 0 & 0 & 0 & 1 \\ 10 & -1 & -10 & -10 & -2 & -10.1 \end{bmatrix} z' + \begin{bmatrix} 1 & 1 \\ 0 & 0 \\ 1 & 0 \\ 0 & 0 \\ 0 & 0 \\ 0 & 1 \end{bmatrix} F \\ y &= \begin{bmatrix} 0 & 1 & 0 & 0 & 0 & 0 \\ 0 & -1 & 0 & 0 & 1 & 0 \end{bmatrix} z'\end{aligned}\quad (41)$$

Now, the first state variable is the integral of the combination of inputs F_1 and F_3 .

However, there are three distinct combination of inputs used in the equation: F_1+F_3 , F_1 , and F_3 . This number must be reduced to two input combinations in order to know where the new integrator is to be applied. By defining a mapping G_2 in which row 1 is subtracted from row 2, as shown in (42),

$$\begin{bmatrix} z_1'' \\ z_2'' \\ z_3'' \\ z_4'' \\ z_5'' \\ z_6'' \end{bmatrix} = \begin{bmatrix} 1 & 0 & 0 & 0 & 0 & 0 \\ 0 & 1 & 0 & 0 & 0 & 0 \\ -1 & 0 & 1 & 0 & 0 & 0 \\ 0 & 0 & 0 & 1 & 0 & 0 \\ 0 & 0 & 0 & 0 & 1 & 0 \\ 0 & 0 & 0 & 0 & 0 & 1 \end{bmatrix} \begin{bmatrix} z_1' \\ z_2' \\ z_3' \\ z_4' \\ z_5' \\ z_6' \end{bmatrix}\quad (42)$$

the representation given by (43) results,

$$\dot{z}'' = \begin{bmatrix} 0 & 0 & 0 & 0 & 0 & 0 \\ 1 & 0 & 1 & 0 & 0 & 0 \\ -0.1 & -2 & -10.1 & -10 & -1 & -10 \\ 0 & 3 & 20 & 19.9 & 3 & 20 \\ 0 & 0 & 0 & 0 & 0 & 1 \\ 0 & -1 & -10 & -10 & -2 & -10.1 \end{bmatrix} z'' + \begin{bmatrix} 1 & 0 \\ 0 & 0 \\ 0 & -1 \\ 0 & 0 \\ 0 & 0 \\ 0 & 1 \end{bmatrix} P \quad (43)$$

$$y = \begin{bmatrix} 0 & 1 & 0 & 0 & 0 & 0 \\ 0 & -1 & 0 & 0 & 1 & 0 \end{bmatrix} z''$$

where P is a vector representing the linear combination of inputs F_1 and F_3 given by (44).

$$\begin{bmatrix} P_1 \\ P_2 \end{bmatrix} = \begin{bmatrix} 1 & 1 \\ 0 & 1 \end{bmatrix} \begin{bmatrix} F_1 \\ F_3 \end{bmatrix} \quad (44)$$

Now, the first state variable may be treated as an input to the rest of the states, as given by (45).

$$\begin{bmatrix} \dot{z}_2'' \\ \dot{z}_3'' \\ \dot{z}_4'' \\ \dot{z}_5'' \\ \dot{z}_6'' \end{bmatrix} = \begin{bmatrix} 0 & 1 & 0 & 0 & 0 \\ -2 & -10.1 & -10 & -1 & -10 \\ 3 & 20 & 19.9 & 3 & 20 \\ 0 & 0 & 0 & 0 & 1 \\ -1 & -10 & -10 & -2 & -10.1 \end{bmatrix} \begin{bmatrix} z_2'' \\ z_3'' \\ z_4'' \\ z_5'' \\ z_6'' \end{bmatrix} + \begin{bmatrix} 1 & 0 \\ -0.1 & -1 \\ 0 & 0 \\ 0 & 0 \\ 0 & 1 \end{bmatrix} \begin{bmatrix} z_1'' \\ P_2 \end{bmatrix}$$

$$\begin{bmatrix} y_1 \\ y_2 \end{bmatrix} = \begin{bmatrix} 1 & 0 & 0 & 0 & 0 \\ -1 & 0 & 0 & 1 & 0 \end{bmatrix} \begin{bmatrix} z_2'' \\ z_3'' \\ z_4'' \\ z_5'' \\ z_6'' \end{bmatrix} \quad (45)$$

$$\dot{z}_1'' = P_1$$

The block diagram of (45) is shown in Figure 3, designating w_p as the vector of state-space variables, v_p as the input vector, and the A, B, and C matrices with the subscript ‘p’.

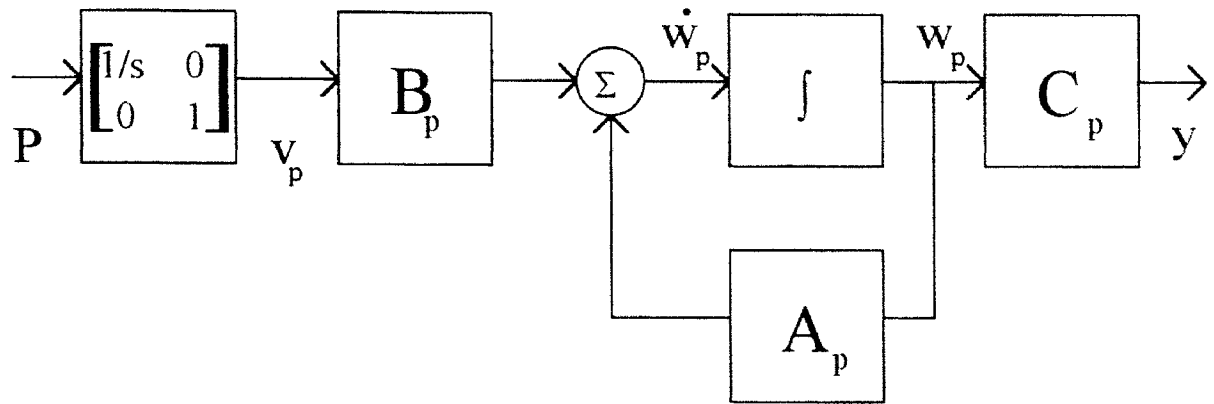


Figure 3. Block Diagram of Un-Augmented System

The free integrator may now be applied in the linear combination shown in Figure 4 to obtain the desired form of v_p .

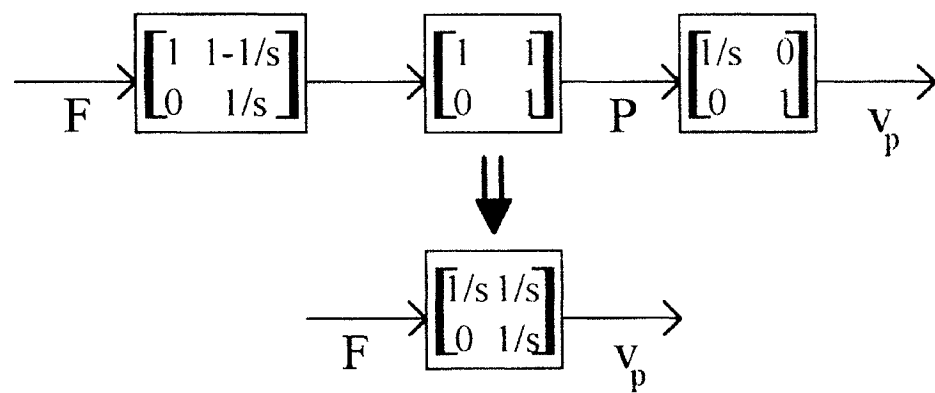


Figure 4. Block Diagram of Free Integrators

The design model, (46), is now defined as in (5).

$$\begin{bmatrix} \dot{v}_p \\ \dot{w}_p \end{bmatrix} = \begin{bmatrix} \emptyset & \emptyset \\ B_p & A_p \end{bmatrix} \begin{bmatrix} v_p \\ w_p \end{bmatrix} + \begin{bmatrix} 1 & 1 \\ 0 & 1 \end{bmatrix} \begin{bmatrix} F_1 \\ F_3 \end{bmatrix} \quad (46)$$

$$\begin{bmatrix} y_1 \\ y_2 \end{bmatrix} = \begin{bmatrix} \emptyset & C_p \end{bmatrix} \begin{bmatrix} v_p \\ w_p \end{bmatrix}$$

Note that the upper submatrix of B is not the identity matrix as in (5) due to the initial free integrator. However, this has no effect on the selection of H since B is not included in the derivation of either G_{KF} or G_{FOL} .

Also, notice that the inputs and outputs of this state-space representation are the same as those for the original system. Furthermore, these inputs and outputs are the only connection between the MBC and the plant. This is important, since it means that the gain matrices to be developed later do not need to be “mapped back” to get them in a form that can be used with the physical system. In other words, so long as the extra free integrator is placed in the right location in the plant (acting on the sum of F_1 and F_3), then the state-space representation, (46), can be used for the MBC, since the inputs and outputs remain consistent for both the MBC and plant.

The procedure for selecting the L matrix begins with the previously described low and high frequency components. From (19), the low frequency component of L is found to be

$$L_l = \begin{bmatrix} 0.3 & 0.15 \\ 0 & 0.5 \end{bmatrix} \quad (47)$$

For comparison, compute the nominal high frequency component as given by (22):

$$L_{H,nom} = \begin{bmatrix} 1 & 0 \\ 0 & 0 \\ 0 & 0 \\ 1 & 1 \\ 0 & 0 \end{bmatrix} \quad (48)$$

The complete L matrix is given by

$$L_{\text{nom}} = \begin{bmatrix} 0.3 & 0.15 \\ 0 & 0.5 \\ 1 & 0 \\ 0 & 0 \\ 0 & 0 \\ 1 & 1 \\ 0 & 0 \end{bmatrix} \quad (49)$$

Selecting an initial value of $\mu = 0.01$ (to ensure that the approximation given by (12) still holds) with the FARE, (10), yields

$$H_{\text{nom}} = \begin{bmatrix} 2.5009 & 2.2351 \\ -1.3129 & 4.8246 \\ 10.8728 & 0.0333 \\ 6.6090 & -0.2000 \\ -14.9701 & -1.5980 \\ 10.9061 & 9.9822 \\ 7.7674 & 1.5265 \end{bmatrix} \quad (50)$$

Using (50), along with A and C from (46), the singular values of G_{KF} were computed and are shown in Figure 5. The crossover frequency is already about 10 rad/sec, so no further modifications are needed. If this were not the case, it would simply be a matter of changing μ (shifting the plot up or down) until the desired crossover frequency was achieved.

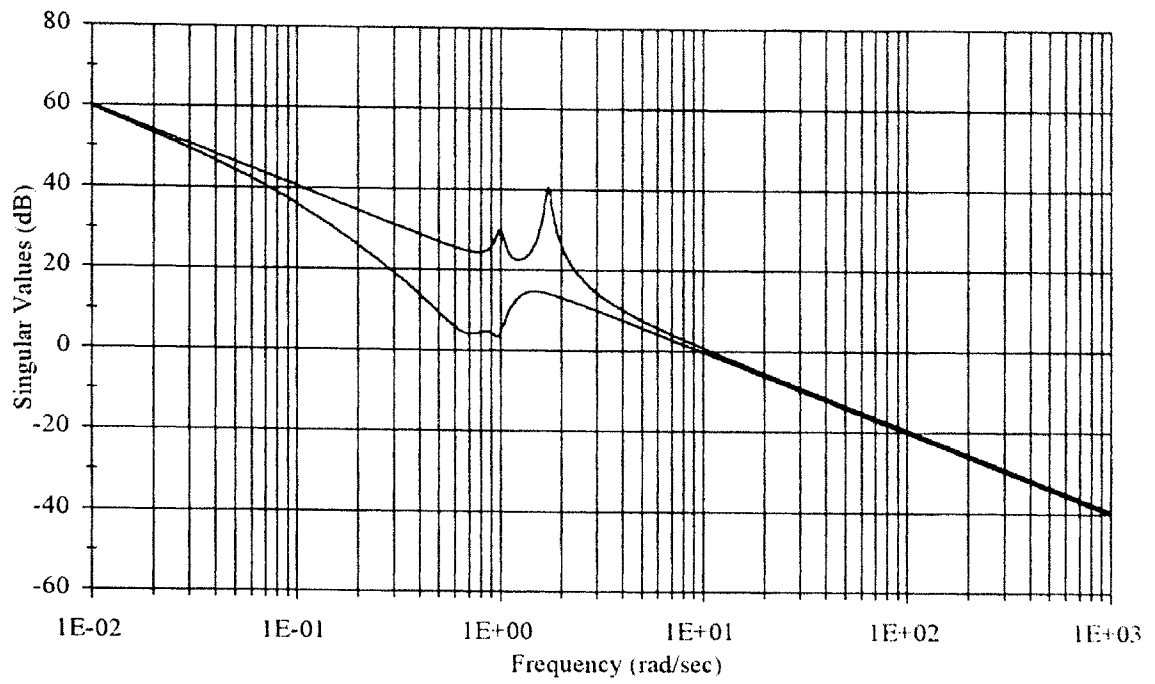


Figure 5. Singular Values of Filter Loop using Nominal H

Now, compute the improved high frequency component of the L matrix using (30).

$$\mathbf{L}_{11,imp} = \begin{bmatrix} 1 & 0 \\ -0.3 & -0.15 \\ 0 & 0 \\ 1 & 1 \\ 0 & 0 \end{bmatrix} \quad (51)$$

The complete L matrix is thus given by (52)

$$\mathbf{L}_{imp} = \begin{bmatrix} 0.3 & 0.15 \\ 0 & 0.5 \\ 1 & 0 \\ -0.3 & -0.15 \\ 0 & 0 \\ 1 & 1 \\ 0 & 0 \end{bmatrix} \quad (52)$$

and the resulting H matrix by (53).

$$H_{\text{imp}} = \begin{bmatrix} 3 & 1.5 \\ 0 & 5 \\ 10 & 0 \\ -3 & -1.5 \\ 0 & 0 \\ 10 & 10 \\ 0 & 0 \end{bmatrix} \quad (53)$$

The singular values of the loop transfer function for this filter gain matrix, shown in Figure 6, exhibit the behavior of a first order Bode plot of $1/s$. As with H_{nom} , the singular value plot using H_{imp} already has the desired crossover frequency, so no changes are needed.

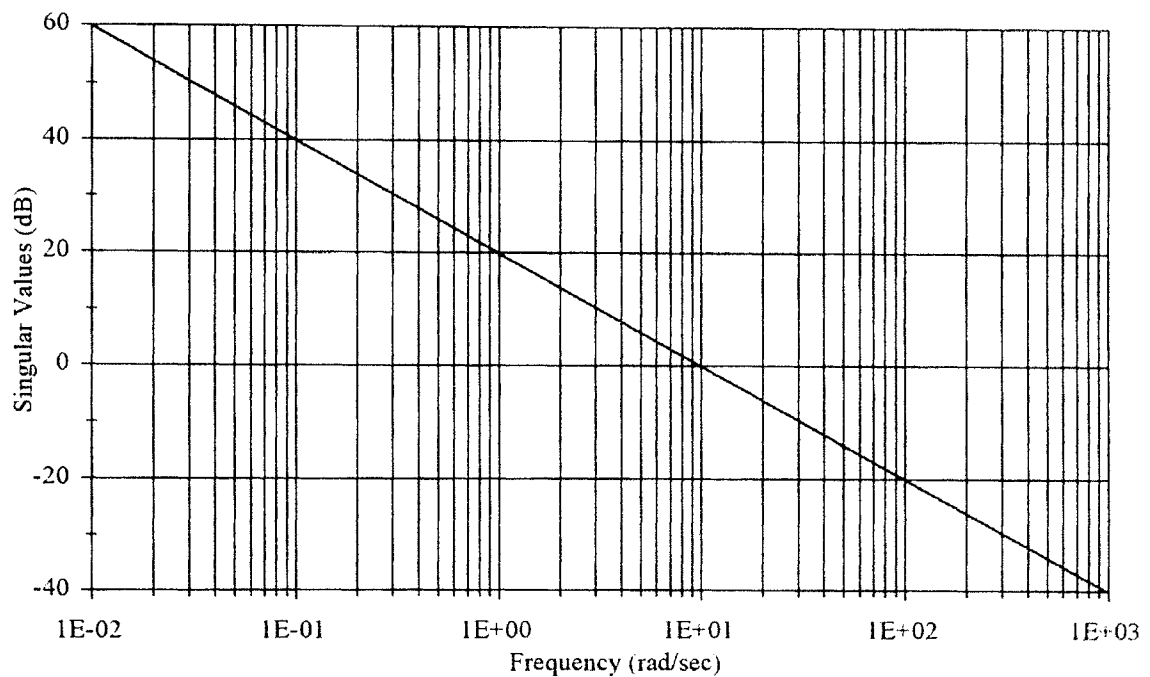


Figure 6. Singular Values of Filter Loop using Improved H

In any case, when the K matrix is selected as per LQG/LTR methodology, the time responses of the system exhibit a much faster, much smoother response with the improved H than with the nominal H. This is illustrated by the time responses to the reference command input $[1 \ 1]'$ shown in Figures 7 and 8, where the free parameter in computing K was chosen to be 10^{-8} .

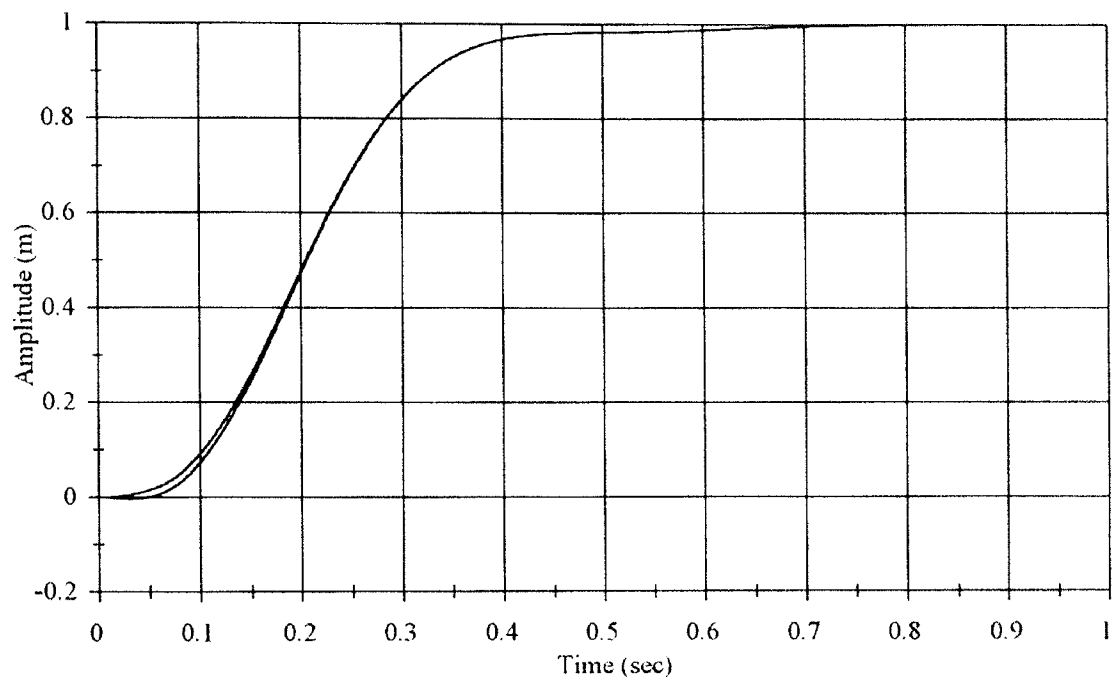


Figure 7. Transient Response of System using Improved H

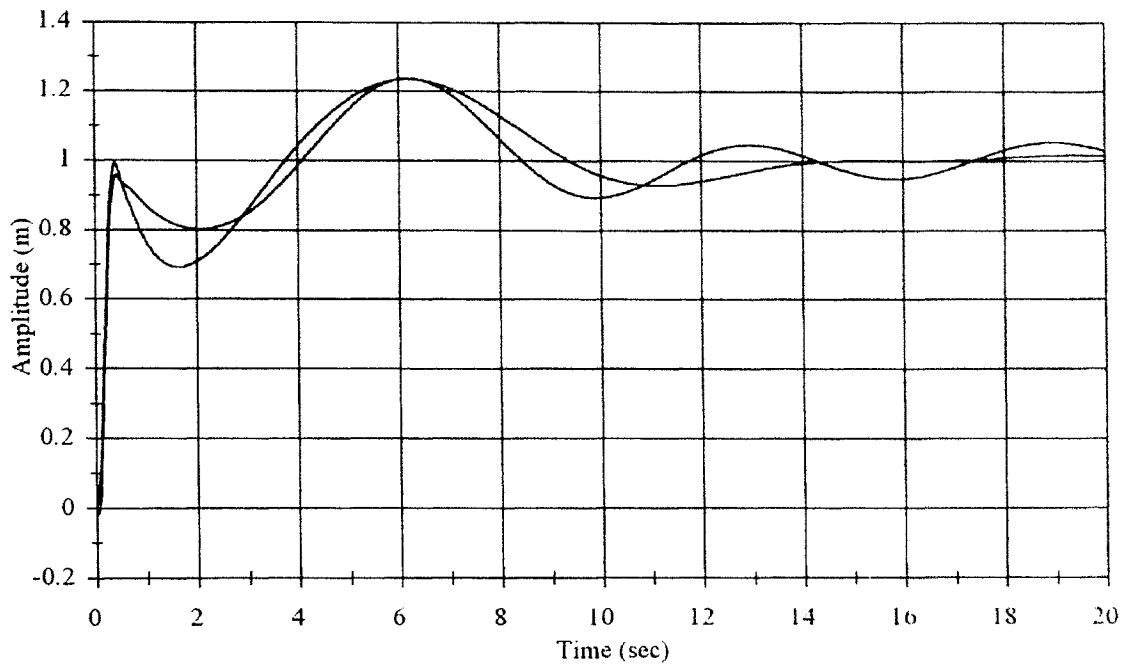


Figure 8. Transient Response of System using Nominal H

It is interesting to note that the control forces needed with the improved H (Figure 9) were actually about 5% smaller than those used with the nominal H (Figure 10). Perhaps this is explained by recognizing the fact that the K matrix for both cases is identical (using the same value for the free parameter), since its calculation is independent of the value of H. The improved H matrix is effectively performing pole/zero cancellation (which will be shown momentarily), thus minimizing the effects of the resonant frequencies. Therefore, the disturbances which must be controlled are minimized as well, such that the control signal leaving K will be smaller.

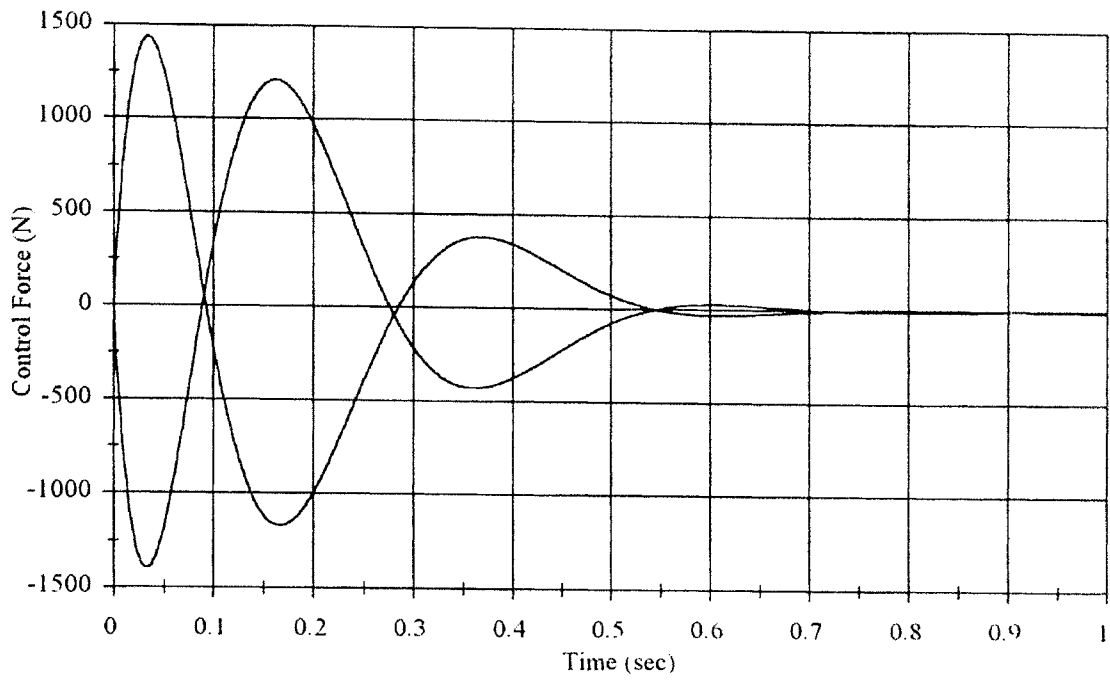


Figure 9. Transient Behavior of Control Forces using Improved H

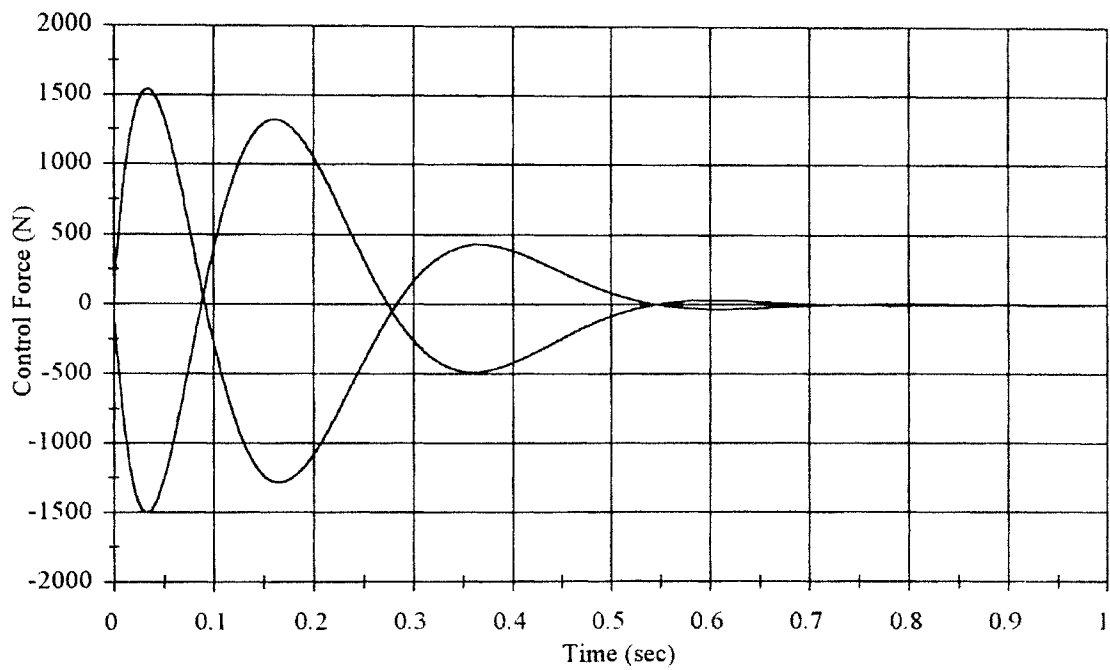


Figure 10. Transient Behavior of Control Forces using Nominal H

Before proceeding to the next example, consider how the filter gain matrix is driving the system to a $1/s$ form. If the filter loop, G_{KF} , is computed symbolically and without canceling terms, the transfer function matrix elements shown in (54) result.

$$\begin{aligned}
 G_{KF_{11}}(s) &= \frac{10s(s+0.1)(s^2+0.1s+3)(s^2+0.1s+1)}{s^2(s+0.1)(s^2+0.1s+3)(s^2+0.1s+1)} \\
 G_{KF_{21}}(s) &= \frac{(6.2 \cdot 10^{-15})(s+29.5)(s-0.32)(s+0.14)(s+5.1 \cdot 10^{-8})}{s^2(s+0.1)(s^2+0.1s+3)(s^2+0.1s+1)} \\
 G_{KF_{12}}(s) &= \frac{(1.2 \cdot 10^{-14})(s+7.3)(s+3.8)(s^2+0.024s+0.96)(s^2+0.018s+0.0037)}{s^2(s+0.1)(s^2+0.1s+3)(s^2+0.1s+1)} \\
 G_{KF_{22}}(s) &= \frac{10s(s+0.1)(s^2+0.1s+3)(s^2+0.1s+1)}{s^2(s+0.1)(s^2+0.1s+3)(s^2+0.1s+1)}
 \end{aligned} \tag{54}$$

The diagonal elements of the matrix (subscripts '11' and '22') reduce to $10/s$ through pole zero cancellation. Recall that the procedure did not attempt to achieve the free integrator form through pole/zero cancellation directly, but that this effect resulted from the LQG filter gain matrix selection process (as did the gain of 10 for proper crossover frequency.) In contrast, the poles and zeros of the off-diagonal elements show no correlation at all. Instead, the design process combines the elements of the $C(sI-A)^{-1}$ matrix in such a way as to drive the sum to a very small number. It can be seen that this also effectively reduces the MIMO system to a set of SISO systems. Thus, SISO design tools such as root locus can be used to predict rise time and other parameters for these individual loops.

The presence of modeling errors, however, would create mismatch between the poles of the system and the cancelling zeros. The Kalman Filter process of selecting the H matrix does provide some stability robustness guarantees for both the nominal and improved methods. A more relevant issue is how the time response of a system is affected

by such modeling errors. Specifically, will the modeling errors create such a degree of pole/zero mismatch that the improved H shows no better performance than the nominal H?

To help address this question, modeling errors were introduced in the previous system. Specifically, mass 1 was treated as if it were actually 1.25 kg (i.e., the model value underestimated the actual value by 25%). Simulations were run to compare the performance of both the nominal and improved controllers to a $[1 \ -1]^T$ reference input. Using the nominal H, the time responses using the accurate model were plotted in Figure 11, and the time responses for the faulty model are shown in Figure 12.

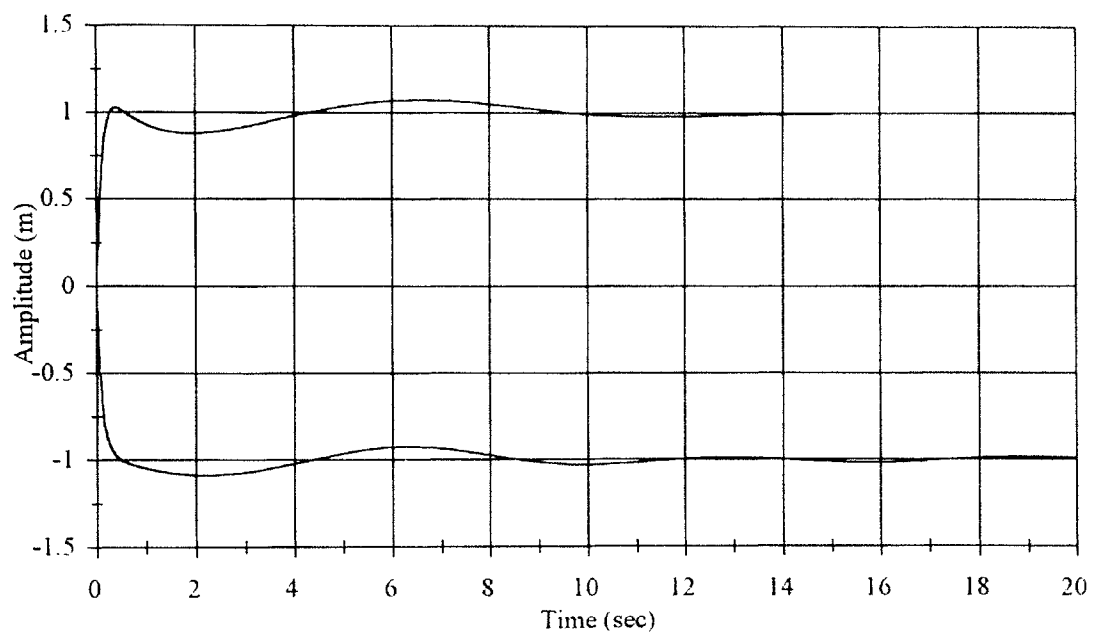


Figure 11. Transient Response using Nominal H with Accurate Model

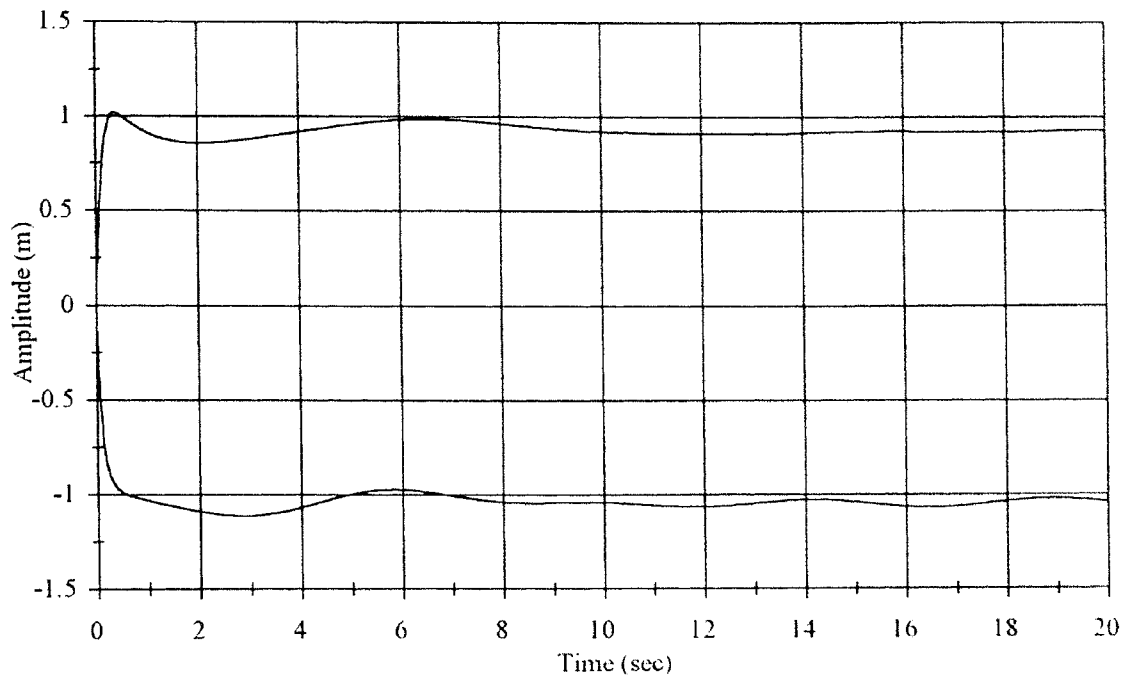


Figure 12. Transient Response using Nominal H with Faulty Model

Similarly, the time responses using the improved H are shown in Figures 13 and 14.

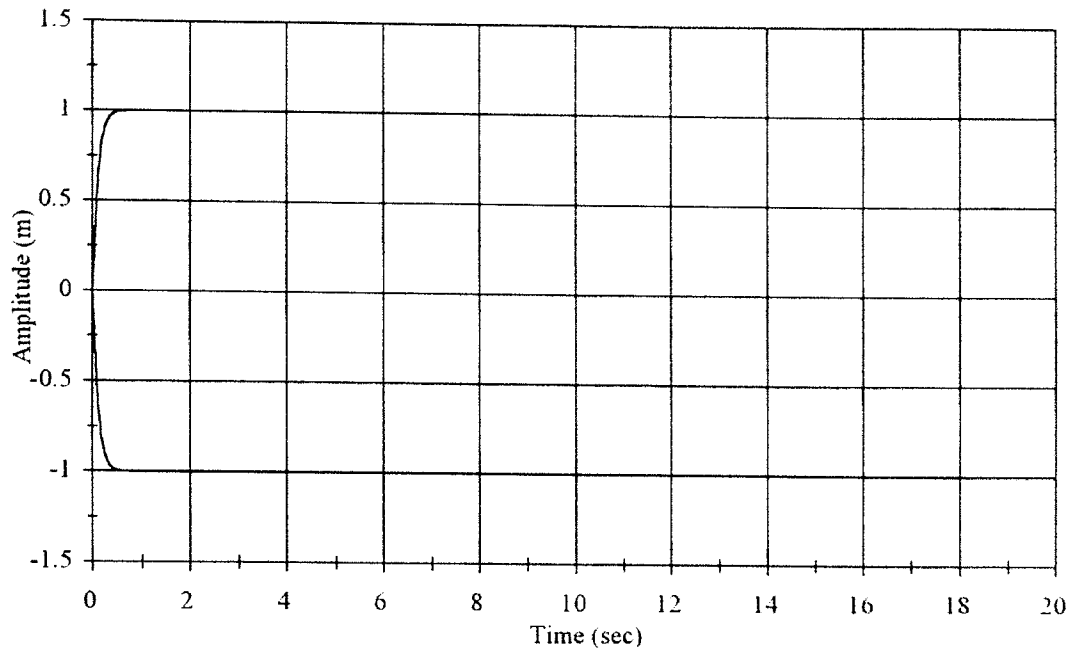


Figure 13. Transient Response using Improved H with Accurate Model

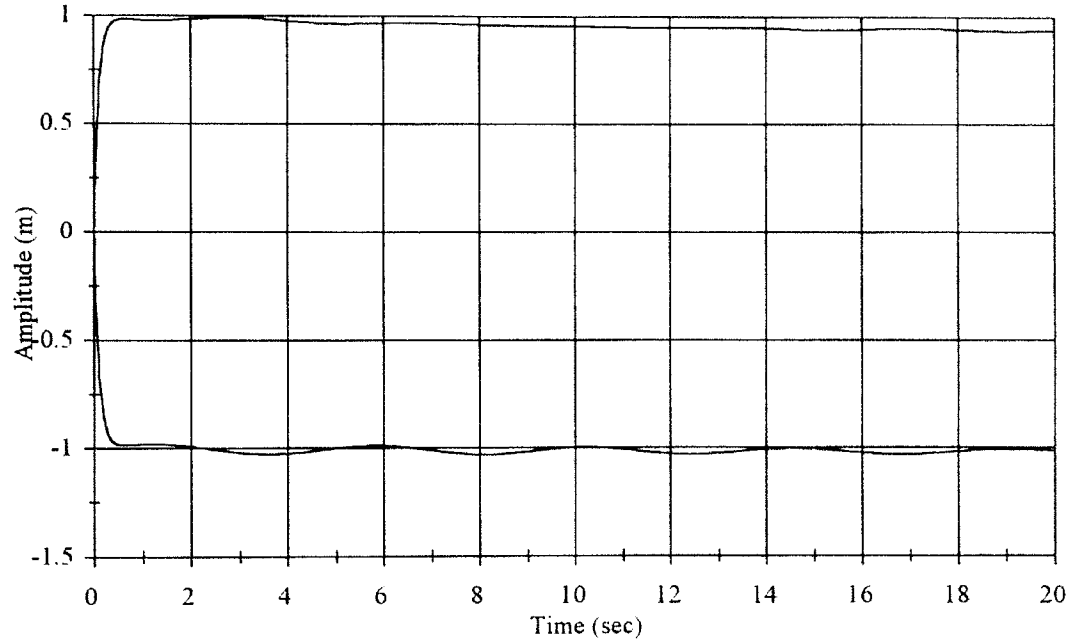


Figure 14. Transient Response using Improved H with Faulty Model

As can be seen from Figures 11 and 13, the improved H shows marked improvement over the nominal H when the model is accurate. When the controllers are designed using the faulty model, both show a relatively fast oscillation on the lower trace (relative position of mass 3 to mass 1), while the upper trace (absolute position of mass 1) shows what appears to be a steady-state error, but is actually a slowly decaying oscillation. However, the improved H response still shows less overshoot and smaller oscillations about the set point than the nominal H response.

While this simple comparison cannot answer all questions about the robustness of the new H, it does seem to indicate that its desirable properties of rise time, settling time, and overshoot are not completely lost in the presence of modeling errors. A more thorough analysis would need to be taken on a case by case basis, as eventually there will be some magnitude of modeling error which will drive both controllers unstable. In any case, it appears that for reasonable errors the improved H still provides a better response.

Example 2: Lightly-Damped Rotating Arm

The previous example illustrated the use of Method 2. This example will show how to use Method 1. Consider a lightly damped rotating arm driven by an electric motor, as might be found in a high-density disk drive, in which the voltage supplied to the motor is the input to the system and the position of the arm is the output (SISO). Assume it has been determined through experimentation that the system has four distinct poles: the first being a free integrator, the second a first order pole at -0.1 , and the third a lightly-damped,

second-order pole with a natural frequency of 8000 rad/sec and a damping ratio of 0.1.

The transfer function of the system, with unity gain, is given by (55).

$$G(s) = 1/s(s+1)[(s^2 - 8000^2) + (0.2s - 8000) + 1] \quad (55)$$

The control canonical form of the state-space representation of (55) is shown in (56), with the singular value plot (Bode diagram) is displayed in Figure 15.

$$\begin{aligned} A_n &= \begin{bmatrix} -1601 & -6.40016 \cdot 10^7 & -6.4 \cdot 10^7 & 0 \\ 1 & 0 & 0 & 0 \\ 0 & 1 & 0 & 0 \\ 0 & 0 & 1 & 0 \end{bmatrix} \\ B_n &= \begin{bmatrix} 1 \\ 0 \\ 0 \\ 0 \end{bmatrix} \\ C_n &= [0 \ 0 \ 0 \ 6.4 \cdot 10^7] \\ D_n &= [0] \end{aligned} \quad (56)$$

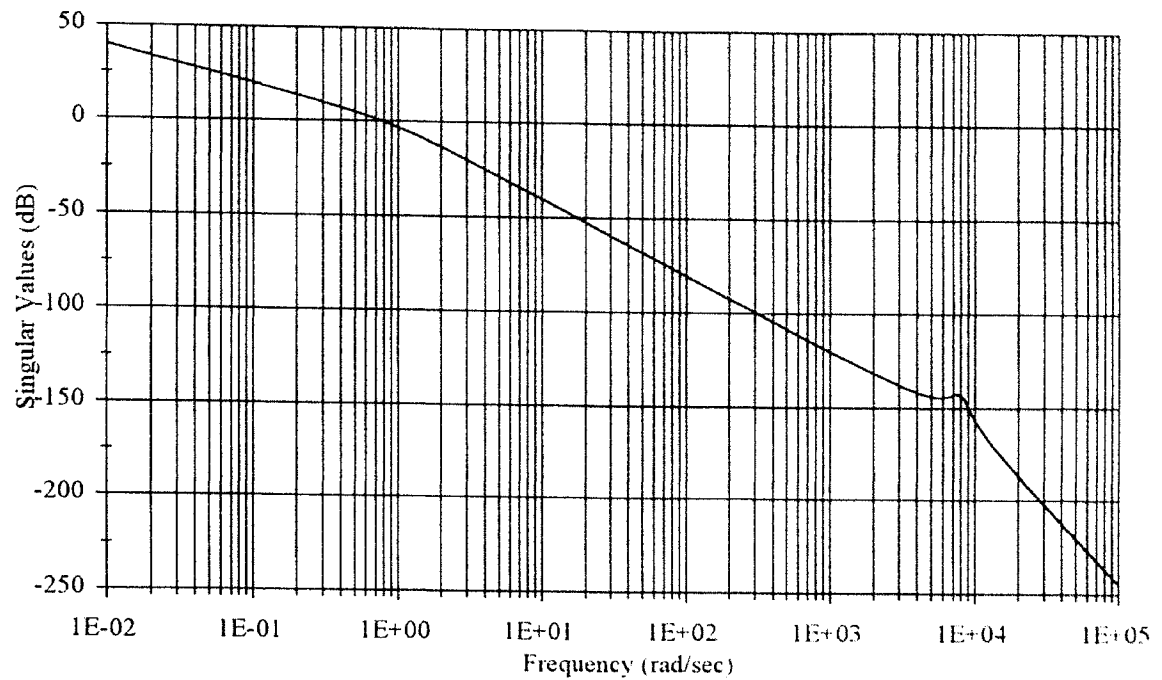


Figure 15. Singular Values of Nominal Plant

Suppose that a LQG/LTR control scheme is to be developed for this system, and that the requirements are as follows:

- zero steady-state error,
- crossover frequency of 600 to 1300 Hz.

The first requirement will be met if the target loop transfer function is at least type one, and the second can be achieved by adjusting the free parameter, μ . Since this is a SISO system, then only one free integrator will be required to make the system type 1. As was indicated earlier, one free integrator already exists, so the only thing left to do is to isolate it as in Example 1.

The mapping shown in (57) will separate the free integrator so that it may be removed.

$$\begin{bmatrix} z_1 \\ z_2 \\ z_3 \\ z_4 \end{bmatrix} = \begin{bmatrix} 1 & 1601 & 6.40016 \cdot 10^7 & 6.4 \cdot 10^7 \\ 0 & 1 & 0 & 0 \\ 0 & 0 & 1 & 0 \\ 0 & 0 & 0 & 1 \end{bmatrix} \begin{bmatrix} x_1 \\ x_2 \\ x_3 \\ x_4 \end{bmatrix} \quad (57)$$

This mapping essentially replaces x_1 with a combination of the rows so that the first row of the new A matrix will be zero. If the above mapping matrix is labeled as G_1 , then the modified plant matrices are given by (58).

$$\begin{aligned} \dot{z} &= GA_n G^{-1} z + GB_n u \\ y &= C_n G^{-1} z \end{aligned} \quad (58)$$

These new plant matrices are

$$\begin{aligned} A'_n &= \begin{bmatrix} 0 & 0 & 0 & 0 \\ 1 & -1601 & -6.40016 \cdot 10^7 & -6.4 \cdot 10^7 \\ 0 & 1 & 0 & 0 \\ 0 & 0 & 1 & 0 \end{bmatrix} \\ B'_n &= \begin{bmatrix} 1 \\ 0 \\ 0 \\ 0 \end{bmatrix} \\ C'_n &= [0 \ 0 \ 0 \ 6.4 \cdot 10^7] \\ D'_n &= [0] \end{aligned} \quad (59)$$

As with the previous example, the first state variable could be pulled out to leave a third order system with a separate free integrator. However, it is easier to simply notice that these matrices are already of the form of (6), where

$$\begin{aligned}
\mathbf{A}_p &= \begin{bmatrix} -1601 & -6.40016 \cdot 10^7 & -6.4 \cdot 10^7 \\ 1 & 0 & 0 \\ 0 & 1 & 0 \end{bmatrix} \\
\mathbf{B}_p &= \begin{bmatrix} 1 \\ 0 \\ 0 \end{bmatrix} \\
\mathbf{C}_p &= [0 \quad 0 \quad 6.4 \cdot 10^7]
\end{aligned} \tag{60}$$

First, apply the standard method of computing the L matrix, using (19) and (22).

This results in (61)

$$\mathbf{L} = \begin{bmatrix} 1 \\ 0 \\ 0 \\ 1.5625 \cdot 10^{-8} \end{bmatrix} \tag{61}$$

where the first element is L_I and the last three form L_{II} . Using a value for μ of 0.01 results in the following value for H.

$$\mathbf{H} = \begin{bmatrix} 1 \\ 3.3382 \cdot 10^{-13} \\ -1.7156 \cdot 10^{-17} \\ 1.5625 \cdot 10^{-7} \end{bmatrix} \tag{62}$$

Now, the gain matrix will be computed using Method 1. The first step is to compute the null vectors of C_p , which are the columns of the following matrix, N_1 .

$$\mathbf{N}_1 = \begin{bmatrix} 0 & -1 \\ 1 & 0 \\ 0 & 0 \end{bmatrix} \tag{63}$$

Next, the matching frequency must be selected. Arbitrarily, the resonant frequency of 8000 is chosen for ω_1 . Applying this frequency, plus the nominal value of L_I and L_{II} from (60) to (26), then computing the pseudoinverse yields the following value for M_1 .

$$\mathbf{M}_1 = \begin{bmatrix} 3.2927 \cdot 10^{-26} - j1.6464 \cdot 10^{-25} \\ -2.0580 \cdot 10^{-29} + j2.5725 \cdot 10^{-33} \end{bmatrix} \quad (64)$$

Generally, the elements of the mapping matrix will not be this small. The reason for the answer shown here will become clear momentarily. First, though, continue with the procedure by computing the new null vector, \mathbf{N}_2 , using (27).

$$\mathbf{N}_2 = \begin{bmatrix} 2.4052 \cdot 10^{-5} - j1.2019 \cdot 10^{-4} \\ 1.000 + j1.8771 \cdot 10^{-25} \end{bmatrix} \quad (65)$$

Next, arbitrarily select 100 rad/sec to serve as ω_2 . Using (28) to solve for \mathbf{M}_2 gives

$$\mathbf{M}_2 = \begin{bmatrix} -1.7607 \cdot 10^{-16} + j3.3154 \cdot 10^{-17} \end{bmatrix} \quad (66)$$

Finally, (29) gives the “improved” value for \mathbf{L} .

$$\mathbf{L} = \begin{bmatrix} 1.000 \\ 1.7607 \cdot 10^{-16} - j3.3154 \cdot 10^{-17} \\ -2.5023 \cdot 10^{-22} + 2.1959 \cdot 10^{-20} \\ 1.5625 \cdot 10^{-8} \end{bmatrix} \quad (67)$$

which, for all practical purposes, is the same as equation (61). In this case, then, the null vectors did not provide any additional improvement to the solution, resulting in the small values of the mapping matrices’ elements. It should be noted that this does not appear to be a general result for all SISO systems, but that some feature of the matrix structure of this system caused this unexpected result. In any case, the singular values of the target loop transfer function are shown in Figure 16.

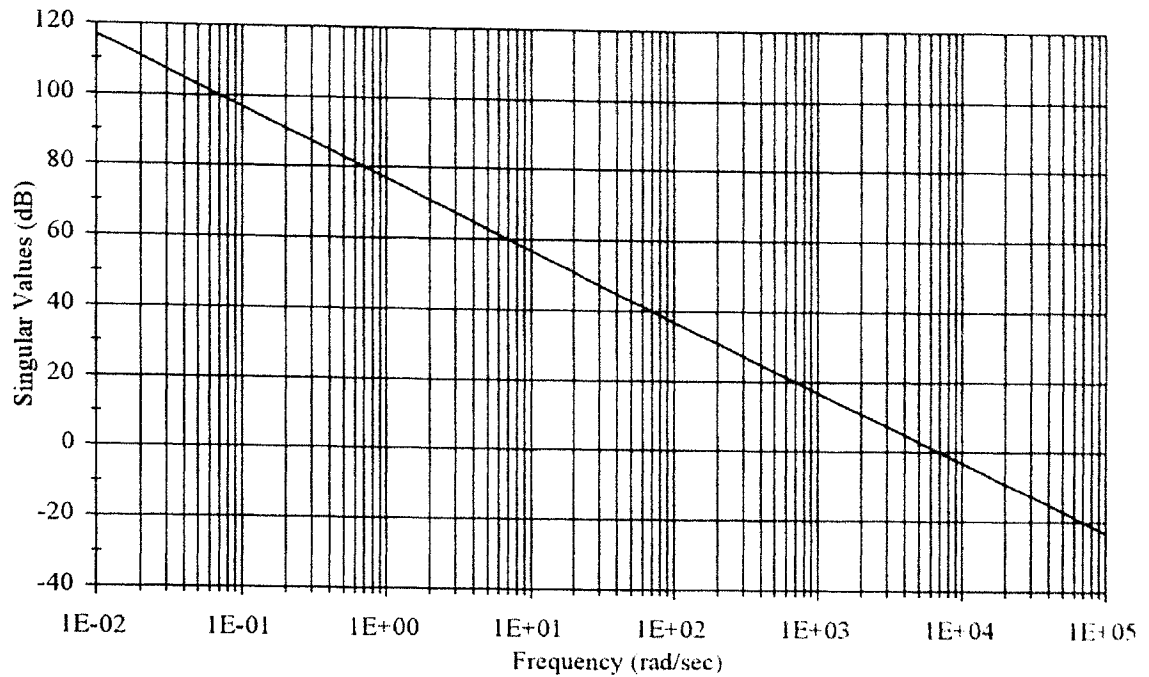


Figure 16. Singular Values of Target Loop Transfer Function

In this plot, the H matrix was computed using a value of $2 \cdot 10^{-8}$ for μ to obtain a crossover frequency in the desired range (1130 Hz):

$$H = \begin{bmatrix} 7.0711 \cdot 10^3 \\ -2.4374 \cdot 10^{-12} \\ 8.2129 \cdot 10^{-16} \\ 1.1049 \cdot 10^{-4} \end{bmatrix} \quad (68)$$

Notice that in (68), the first element of the matrix is seven orders of magnitude larger than any of the others. Since it is most likely impractical to have such comparatively small gains, then it might be interesting to see what effect zeroing these out has on the loop shape. The singular values under this condition is shown in Figure 17.

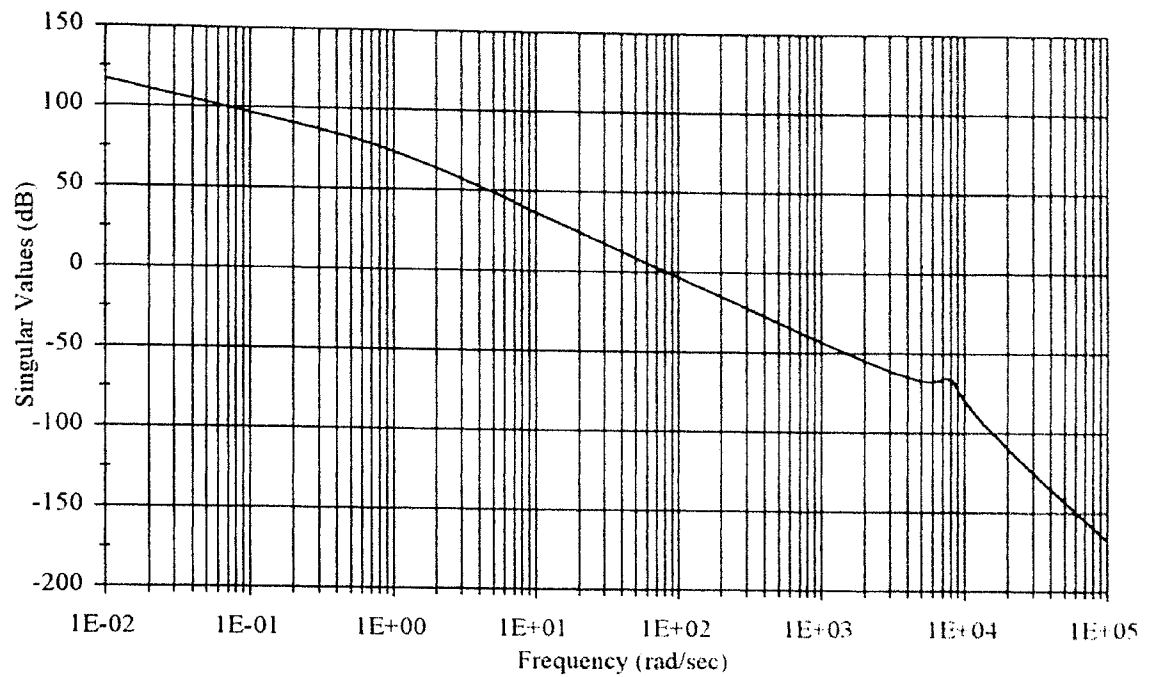


Figure 17. Singular Values of Target Loop using Approximate H

The singular values shown in Figure 17 are not that different than those of Figure 15, except that they have been shifted up due to the gain effect of μ . This result leads to the question of how the transient response of the system varies with different “accuracy’s” of the filter gain matrix. Figure 18 shows the transient response of the system to a unit step reference input using (68) as the filter matrix.

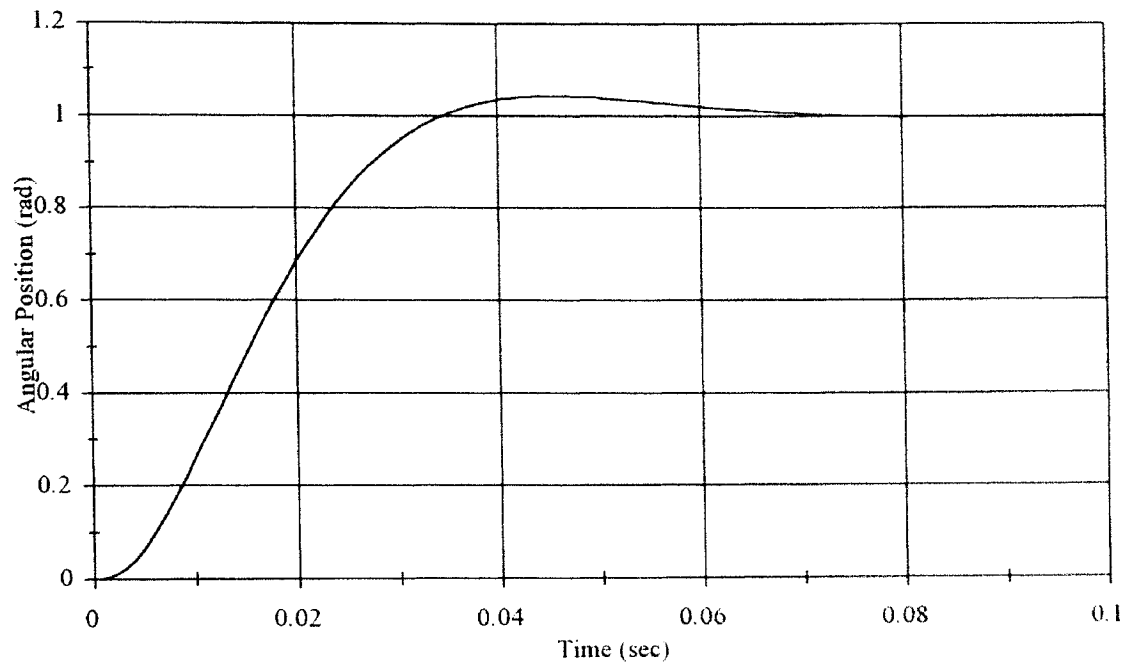


Figure 18. Transient Response of System using Exact Filter Matrix

Figure 19 shows the time response to the same input if all but the first element in the H matrix is zeroed out. In both figures, the control gain matrix, K, was selected using equations 8 and 9, with a value of 10^{-8} for the free parameter, ρ :

$$K = [140.44 \quad 9861.2 \quad 1.5748 \cdot 10^7 \quad 6.3101 \cdot 10^{11}] \quad (69)$$

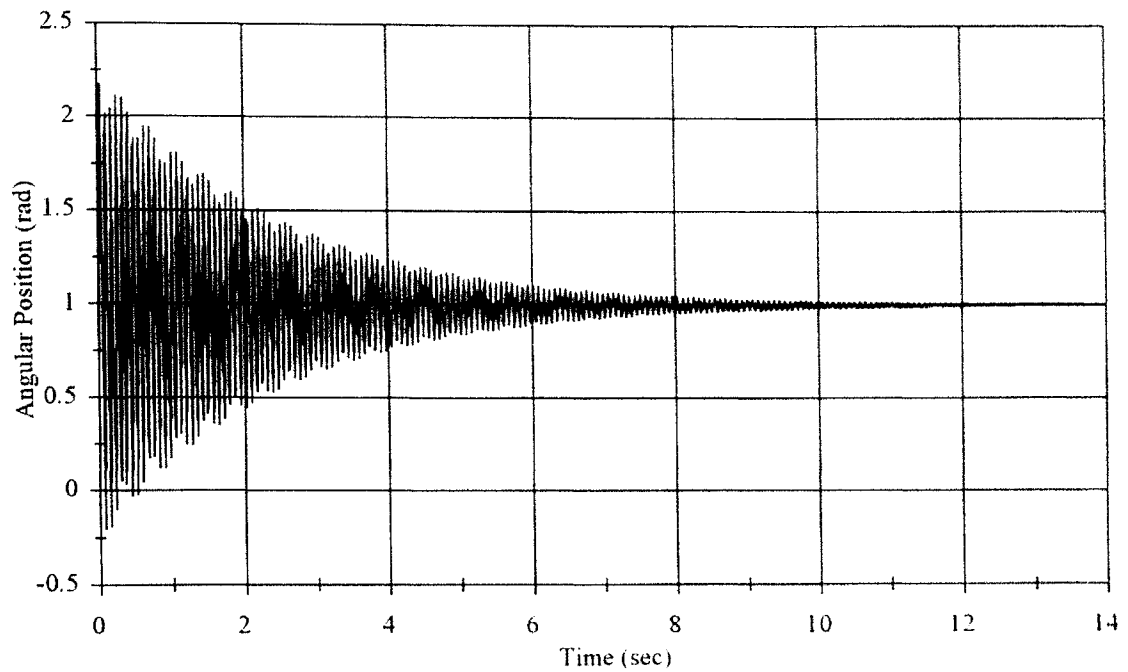


Figure 19. Transient Response of System using Approximate II

Notice that the effects of the resonant pole are clearly present in Figure 19, while the response in Figure 18 is very smooth and settles out to the steady-state value quickly. Therefore, it is seen that even small gains can be extremely important to the resulting behavior of the system (although the degree of sensitivity will vary). However, this is more of a limitation of the hardware and software used to effect the control scheme than of the LQG/LTR process, itself.

CHAPTER V

CONCLUSIONS

The technique for computing the Kalman Filter matrix presented in this paper offers a significant improvement over the previous method. The time responses to reference inputs are faster and smoother than with the nominal Kalman Filter gain matrix, while at the same time using less control effort. As mentioned earlier, the improved H is actually attempting to perform pole/zero cancellation on the original system dynamics. It would therefore be interesting to see how modeling errors might affect the transient response of the system. Regardless of the magnitude of these errors, however, it is reasonable to assume that better results will be obtained by attempting to minimize their effects using the improved H than by leaving them untouched using the standard method.

BIBLIOGRAPHY

Arthur, A., 1972, *Regression and the Moore-Penrose Pseudoinverse*, New York: Academic Press, Inc.

Kwakernaak, H., and Sivan, R., 1972, *Linear Optimal Control Systems*, New York: John Wiley and Sons, Inc.

Kailath, T., 1980, *Linear Systems*, Englewood Cliffs, NJ: Prentice-Hall.

Doyle, J. C., and Stein, G., 1981, "Multivariable Feedback Design: Concepts for a Classical/Modern Synthesis," *IEEE Transactions on Automatic Control*, Vol. AC-26, No. 1, pp 4-16.

Birdwell, J. D., Athans, M. T., Strunce, R., Bly, S. A., Herget, C. J., Laub, A. J., Cockett, R., Heller, R. W., Heath, M. T., and Stovall, J. P., 1984, "Issues in the Design of a Computer-Aided Systems and Control Analysis and Design Environment (CASCADE)," ORNL/TN--9038, Oak Ridge National Laboratory, Oak Ridge, TN.

Martin, R. J., Valvani, L., and Athans, M., 1986, "Multivariable Control of a Submersible using the LQG/LTR Design Methodology," reprinted from *Proceedings American Control Conference*, Seattle, WA.

Birdwell, J. D., and Laub, A. J., 1987, "Balanced singular values for LQR/LTR design," *International Journal of Controls*, Vol. 45, No. 3, pp. 939-950.

Stein, G., and Athans, M., 1987, "The LQG/LTR Procedure for Multivariable Feedback Control Design," *IEEE Transactions on Automatic Control*, Vol. AC-32, No. 2, pp.105-114.

Brogan, W. L., 1991, *Modern Control Theory*, 3rd ed., Englewood Cliffs, NJ:
Prentice Hall.

APPENDIX

Derivation of Formula

Substituting (17) into (15) and multiplying through by s yields (70).

$$\mathbf{I} = -\mathbf{C}_p (\mathbf{sI} - \mathbf{A}_p)^{-1} \mathbf{B}_p (\mathbf{C}_p \mathbf{A}_p^{-1} \mathbf{B}_p)^{-1} + \mathbf{sC}_p (\mathbf{sI} - \mathbf{A}_p)^{-1} \mathbf{L}_{II} \quad (70)$$

The inverse of any matrix is given by its adjoint divided by its determinant, as shown for the matrix $(\mathbf{sI} - \mathbf{A})$ in (71).

$$(\mathbf{sI} - \mathbf{A})^{-1} = \text{Adj}(\mathbf{sI} - \mathbf{A}) / \det(\mathbf{sI} - \mathbf{A}) \quad (71)$$

Kailath (1980, 656-7) gives the following formulas for this adjoint and determinant:

$$\det(\mathbf{sI} - \mathbf{A}) = s^n + a_1 s^{n-1} + a_2 s^{n-2} + \dots + a_{n-1} s + a_n \quad (72)$$

$$\text{Adj}(\mathbf{sI} - \mathbf{A}) = \left[\mathbf{I} s^{n-1} + (\mathbf{A} + a_1 \mathbf{I}) s^{n-2} + \dots + (\mathbf{A}^{n-1} + a_1 \mathbf{A}^{n-2} + \dots + a_{n-1} \mathbf{I}) \right] \quad (73)$$

Substituting (71), (72), and (73) into (70) then multiplying through by the determinant results in (74).

$$\begin{aligned} (s^n + a_1 s^{n-1} + a_2 s^{n-2} + \dots + a_{n-1} s + a_n) \mathbf{I} = \\ -\mathbf{C}_p \left[\mathbf{I} s^{n-1} + (\mathbf{A}_p + a_1 \mathbf{I}) s^{n-2} + \dots + (\mathbf{A}_p^{n-1} + a_1 \mathbf{A}_p^{n-2} + \dots + a_{n-1} \mathbf{I}) \right] \mathbf{B}_p (\mathbf{C}_p \mathbf{A}_p^{-1} \mathbf{B}_p)^{-1} \\ + \mathbf{C}_p \left[\mathbf{I} s^n + (\mathbf{A}_p + a_1 \mathbf{I}) s^{n-1} + \dots + (\mathbf{A}_p^{n-1} + a_1 \mathbf{A}_p^{n-2} + \dots + a_{n-1} \mathbf{I}) s \right] \mathbf{L}_{II} \end{aligned} \quad (74)$$

For (74) to hold, the coefficients of the powers of s must match for a given \mathbf{L}_{II} matrix.

$$[s^n]: \quad \mathbf{I} = \mathbf{C}_p \mathbf{L}_{II} \quad (75)$$

$$[s^{n-1}]: \quad a_1 \mathbf{I} = -\mathbf{C}_p \mathbf{B}_p (\mathbf{C}_p \mathbf{A}_p^{-1} \mathbf{B}_p)^{-1} + \mathbf{C}_p (\mathbf{A}_p + a_1 \mathbf{I}) \mathbf{L}_{II} \quad (76)$$

Expanding (76):

$$\mathbf{a}_1 \mathbf{I} = -\mathbf{C}_p \mathbf{B}_p (\mathbf{C}_p \mathbf{A}_p^{-1} \mathbf{B}_p)^{-1} + \mathbf{C}_p \mathbf{A}_p \mathbf{L}_{H1} + \mathbf{a}_1 \mathbf{C}_p \mathbf{L}_{H1} \quad (77)$$

Substituting (75) into (77) then canceling like terms gives (78)

$$\emptyset = \mathbf{C}_p \left[\mathbf{A}_p \mathbf{L}_{H1} - \mathbf{B}_p (\mathbf{C}_p \mathbf{A}_p^{-1} \mathbf{B}_p)^{-1} \right] \quad (78)$$

Thus, the term in braces is identity zero (and so is the right hand side) if \mathbf{L}_{H1} is chosen to be

$$\mathbf{L}_{H1} = \mathbf{A}_p^{-1} \mathbf{B}_p (\mathbf{C}_p \mathbf{A}_p^{-1} \mathbf{B}_p)^{-1} \quad (79)$$

Proof of Exact Solution

Equation (79) can be shown to be a solution to (74) by matching coefficients of powers of s individually. Alternatively, (79) can be substituted directly into (74).

$$\begin{aligned} & (s^n + a_1 s^{n-1} + a_2 s^{n-2} + \dots + a_{n-1} s + a_n) \mathbf{I} = \\ & -\mathbf{C}_p \left[\mathbf{I} s^{n-1} + (\mathbf{A}_p + \mathbf{a}_1 \mathbf{I}) s^{n-2} + \dots + (\mathbf{A}_p^{n-1} + \mathbf{a}_1 \mathbf{A}_p^{n-2} + \dots + \mathbf{a}_{n-1} \mathbf{I}) \right] \mathbf{B}_p (\mathbf{C}_p \mathbf{A}_p^{-1} \mathbf{B}_p)^{-1} \\ & + \mathbf{C}_p \left[\mathbf{I} s^n + (\mathbf{A}_p + \mathbf{a}_1 \mathbf{I}) s^{n-1} + \dots + (\mathbf{A}_p^{n-1} + \mathbf{a}_1 \mathbf{A}_p^{n-2} + \dots + \mathbf{a}_{n-1} \mathbf{I}) s \right] \mathbf{A}_p^{-1} \mathbf{B}_p (\mathbf{C}_p \mathbf{A}_p^{-1} \mathbf{B}_p)^{-1} \end{aligned} \quad (80)$$

Collecting coefficients of the powers of s ...

$$\begin{aligned} & (s^n + a_1 s^{n-1} + a_2 s^{n-2} + \dots + a_{n-1} s + a_n) \mathbf{I} = \\ & \mathbf{C}_p \left[\mathbf{A}_p^{-1} s^n + (\mathbf{A}_p \mathbf{A}_p^{-1} + \mathbf{a}_1 \mathbf{A}_p^{-1} - \mathbf{I}) s^{n-1} + (\mathbf{A}_p^2 \mathbf{A}_p^{-1} + \mathbf{a}_1 \mathbf{A}_p \mathbf{A}_p^{-1} + \mathbf{a}_2 \mathbf{A}_p^{-1} - \mathbf{A}_p - \mathbf{a}_1 \mathbf{I}) s^{n-2} \right. \\ & + \dots + (\mathbf{A}_p^{n-1} \mathbf{A}_p^{-1} + \mathbf{a}_1 \mathbf{A}_p^{n-2} \mathbf{A}_p^{-1} + \dots + \mathbf{a}_{n-2} \mathbf{I} + \mathbf{a}_{n-1} \mathbf{A}_p^{-1} - \mathbf{A}_p^{n-2} - \mathbf{a}_1 \mathbf{A}_p^{n-3} - \dots - \mathbf{a}_{n-3} \mathbf{A}_p - \mathbf{a}_{n-2} \mathbf{I}) s \\ & \left. + (-\mathbf{A}_p^{n-1} - \mathbf{a}_1 \mathbf{A}_p^{n-2} - \dots - \mathbf{a}_{n-2} \mathbf{A}_p - \mathbf{a}_{n-1} \mathbf{I}) \right] \mathbf{B}_p (\mathbf{C}_p \mathbf{A}_p^{-1} \mathbf{B}_p)^{-1} \end{aligned} \quad (81)$$

Simplifying...

$$\begin{aligned} & (s^n + a_1 s^{n-1} + a_2 s^{n-2} + \dots + a_{n-1} s + a_n) \mathbf{I} = \\ & \mathbf{C}_p \left[\mathbf{A}_p^{-1} s^n + \mathbf{a}_1 \mathbf{A}_p^{-1} s^{n-1} + \mathbf{a}_2 \mathbf{A}_p^{-1} s^{n-2} + \dots + \mathbf{a}_{n-1} \mathbf{A}_p^{-1} s \right. \\ & \left. + (-\mathbf{A}_p^{n-1} - \mathbf{a}_1 \mathbf{A}_p^{n-2} - \dots - \mathbf{a}_{n-2} \mathbf{A}_p - \mathbf{a}_{n-1} \mathbf{I}) \right] \mathbf{B}_p (\mathbf{C}_p \mathbf{A}_p^{-1} \mathbf{B}_p)^{-1} \end{aligned} \quad (82)$$

The coefficient of s^0 may be rewritten as in (83).

$$\begin{aligned} & (s^n + a_1 s^{n-1} + a_2 s^{n-2} + \dots + a_{n-1} s + a_n) I = \\ & C_p \left\{ A_p^{-1} s^n + a_1 A_p^{-1} s^{n-1} + a_2 A_p^{-1} s^{n-2} + \dots + a_{n-1} A_p^{-1} s \right. \\ & \left. + [a_n I - (A_p^n + a_1 A_p^{n-1} + \dots + a_{n-2} A_p^2 + a_{n-1} A_p + a_n I)] A_p^{-1} \right\} B_p (C_p A_p^{-1} B_p)^{-1} \end{aligned} \quad (83)$$

Kailath (1980, 658) shows that by the Cayley-Hamilton theorem,

$$A_p^n + a_1 A_p^{n-1} + \dots + a_{n-2} A_p^2 + a_{n-1} A_p + a_n I = 0 \quad (84)$$

This reduces (83) to

$$\begin{aligned} & (s^n + a_1 s^{n-1} + a_2 s^{n-2} + \dots + a_{n-1} s + a_n) I = \\ & C_p (A_p^{-1} s^n + a_1 A_p^{-1} s^{n-1} + a_2 A_p^{-1} s^{n-2} + \dots + a_{n-1} A_p^{-1} s + a_n A_p^{-1}) B_p (C_p A_p^{-1} B_p)^{-1} \end{aligned} \quad (85)$$

The inverse of A_p is a common term in the coefficients of the powers of s , such that it may be pulled out to leave a scalar quantity in the parenthesis.

$$\begin{aligned} & (s^n + a_1 s^{n-1} + a_2 s^{n-2} + \dots + a_{n-1} s + a_n) I = \\ & (s^n + a_1 s^{n-1} + a_2 s^{n-2} + \dots + a_{n-1} s + a_n) C_p A_p^{-1} B_p (C_p A_p^{-1} B_p)^{-1} \end{aligned} \quad (86)$$

This simplifies to (87), completing the proof.

$$(s^n + a_1 s^{n-1} + a_2 s^{n-2} + \dots + a_{n-1} s + a_n) I = (s^n + a_1 s^{n-1} + a_2 s^{n-2} + \dots + a_{n-1} s + a_n) I \quad (87)$$

VITA

Brian Dwayne O'Dell

Candidate for the Degree of

Master of Science

Thesis: OBTAINING UNIFORM SINGULAR VALUES OF AUGMENTED
 SYSTEMS USING LQG/LTR

Major Field: Mechanical Engineering

Biographical:

Personal Data: Born in Fort Smith, Arkansas, on August 30, 1971, the son of
 Danny and Melanie O'Dell.

Education: Graduated from Roland High School, Roland, Oklahoma in May 1989;
 received Bachelor of Science degree in Mechanical Engineering from
 Oklahoma State University, Stillwater, Oklahoma in May 1993. Will complete
 the requirements for the Master of Science degree with a major in Mechanical
 Engineering at Oklahoma State University in December 1994.

Experience: Worked as an engineering intern at AES Shady Point, a power plant
 near Panama, Oklahoma, during summer of 1992.

Professional Memberships: American Society of Mechanical Engineers.